Textile Research Journal

Original article

Textile Research Journal
2017, Vol. 87(3) 305–328

DOI: 10.1177/0040517516629146
journals.sagepub.com/home/trj
SAGE

Effect of proportion of carbon fiber content and the dispersion of two fiber types on tensile and compressive properties of intra-layer hybrid composites

Md. Hasan Ikbal and Li Wei

Abstract

Fourteen types of composite laminates—plain carbon/epoxy composite laminate, plain glass/epoxy composite laminate, and 12 carbon fiber–glass fiber/epoxy intra-layer hybrid composite laminates—were made with different relative proportions of the two fiber types and different dispersions. Tensile and compressive mechanical properties were tested and the results were simulated using the ABAQUS/Explicit commercial software package. The relative proportion of carbon fiber content largely affected the tensile and compressive mechanical properties and the so-called hybridization effect, and should be treated as one of the most crucial parameters. Though the degree of dispersion does not significantly affect mechanical performance, it certainly affects the failure modes of the composites. Scanning electron microscopy revealed that under both tensile and compressive loading, the low-elongation carbon fiber failed first, there was a stress drop in the stress–strain diagram, and then the materials continued extending; meaning that the rest of the load was carried by the remaining glass fibers. With a high dispersion of fiber types, composites tend to fail in a more controlled way, i.e. the curves have a plateau region at the end, and catastrophic failure is thereby avoided.

Keywords

hybrid composites, glass fiber, carbon fiber, intralayer hybridization, hybridization effects

Fiber-reinforced polymer (FRP) composites are made by combining a plastic polymer resin (commonly known as the matrix) together with strong reinforcing fibers. The components keep their original form and contribute their own unique properties, which results in a new composite material with enhanced overall performance. Reinforcing polymer material with fibers improves their strength and stiffness. FRP composites have already proven themselves to be increasingly important in various industries, particularly in aerospace, wind energy, sports, and automotive applications. They have an excellent stiffness and strength, with a low density (as compared to steel, and many other metals and alloys) and so are attracting more interest for these weight-sensitive applications. Among the many types of fibers available, carbon and glass fibers are the two most widely used fibers in the fiber-reinforced plastics industry.

Unfortunately, the high modulus or stiffness and strength of carbon composites come at the expense of their limited toughness (very low failure strain). Therefore, like most materials, FRP also faces the ''strength versus toughness'' predicament. Carbon fibers have high strength and stiffness, while glass fibers have moderate strength and low stiffness,[1,2] which means that carbon fibers are low elongation (LE) fibers while glass fibers are high elongation (HE) fibers. The low elongation and relatively low ratio of

Key Laboratory of Textile Science and Technology, Donghua University, China

Corresponding author:
Li Wei, College of Textiles, Donghua University, Shanghai, China, 201620.
Email: liwei@dhu.edu.cn

compressive-to-tensile strength of carbon fiber[3–5] may be a disadvantage for the use of carbon fiber-reinforced polymer (CFRP) composites when utilized as structural members subjected to compressive or flexural loading, or both.

In general, it is believed that when these two fiber types are mixed to reinforce a common polymer matrix, it is possible to obtain a composite with balanced properties. Such composites, when made of two or more reinforcement fibers in a common matrix, are called hybrid composites. Glass fibers and carbon fibers can be mingled to modify and improve the failure strain of CFRP.[6] HE fibers, i.e. glass fibers, increase the level of strain at which cracks propagate through the composites and hence behave like crack arrestors at a micromechanical level.[7]

Hybrid composites can be categorized into intimately mixed, intra-ply, inter-ply, and sandwiched types.[8] The rule-of-mixtures (RoM) approach, which is calculated considering the individual properties and the volume fractions of its constituent types, is a useful means of tentatively estimating the properties of hybrid composites. The hybrid effect, which could be either positive or negative, is calculated based on the positive or negative deviation of a particular mechanical property from the RoM behavior.[9] Many studies have been carried out on the properties of glass and carbon fiber-reinforced hybrid composites.[1,7,8,10–19] Most studies focused on strength.[10,12–16,18] Fu et al.[9] reported that there is no hybrid effect upon the tensile modulus (the tensile modulus obtained from the test follows the RoM), while a positive hybrid effect exists for the flexural modulus. The longitudinal tensile modulus of hybrid composites has been shown to obey a linear rule of mixtures, according to many researchers.[8,11,12,20,21]

According to many researchers, the hybrid effect upon tensile strength is based on a bilinear RoM.[6,8,22] However, considering data reported by Shan and Liao[23] it is seen that a bilinear RoM does not yield a satisfactory prediction. Positive deviation from the bilinear RoM was found in Peijs et al.[24] A hybrid effect on tensile failure strain is reported by many researchers.[7,11,16,17,20,25–29] A typical range of hybrid effect upon failure strain is 10–50%, though some outliers have been reported.[30] From the reports presented by Chamis et al.,[31] Kretsis[8] calculated negative hybrid effects for failure strain down to −66%, which were discarded as being unrealistic values.

Factors that influence the mechanical performance from a reinforcement point of view are length of the fiber, fiber orientation, fiber shape, and fiber material.[32,33] Nonetheless, the overwhelming number of experiments on the importance of dispersion[6,34–38] show that this is also undoubtedly one of the most critical parameters. Experimentally, additional improvements of about 20% in failure strain by increasing dispersion have been reported by many authors.[35,37,38] The relative proportion of both fibers is another crucial parameter for the hybrid effect of hybrid composites. Kretsis[8] showed that when the relative proportion of LE fiber is low, the hybrid effect upon failure strain of the LE fiber composite is larger. Fukunaga et al.[39] also showed that the hybrid effect is greater when the LE fiber content is lower.

In this study, the tensile and compressive properties of unidirectional E-glass and T620S carbon fiber-reinforced epoxy intra-layer hybrid composites were studied using three methods: finite element analysis (FEA), experimental, and scanning electron microscopy. Focus has been given to the effect of the relative proportion of carbon fiber in the mixing ratio upon mechanical properties. The effect of the dispersion of the carbon and glass fibers, while keeping the relative volume fractions of the two fiber types same, upon mechanical performance is also discussed.

Material preparation

Materials and their properties

Toray T620SC-24K-50C carbon and CPIC ECT469L-2400 E-glass fibers were used in this study. Carbon fiber is one of the most commonly used fibers in FRP composites due to its having a very high strength-to-weight ratio and very high stiffness. Glass fiber is one of the most commonly used fibers in polymeric composites. The required interfacial adhesion and bonding between layers of fiber is achieved by using epoxy resin and hardener mixed in a ratio of 10:1. Some major properties of fibers and the resin matrix are given in Table 1.

Sample preparation

Plain carbon and plain glass composite laminates were made using Unidirectional carbon (UD carbon) and Unidirectional glass (UD glass) fabrics, respectively. The intra-layer hybrid configurations of the specimens were made using four types of carbon and glass unidirectional noncrimp hybrid fabrics. The fabrics were produced by a warp knitting technique on a Tricot machine (tows were bound together at an angle of $\pm 60^{\circ}$ using a hot melt yarn of linear density 52.5 Tex and an areal density of 7.2 g/m^2 as knitting yarn). Construction details and areal density of the plies of each type of fabric, with their laminate geometry, are provided in Figure 1. The fabrics were supplied by the Shanghai Jinwei High Performance Fiber Co. Ltd., China.

Samples were prepared and categorized into four groups according to different volume fractions/proportions of the two fiber types (Figure 1). In group I, the

Table 1. Major properties of the constituents

	Major properties				
Material	Density (g/cc)	Strength (MPa)	Modulus (GPa)	Failure strain (%)	Linear density of tow (Tex)
Carbon fiber	1.77	4400	235	1.70	1850
E-glass fiber	2.54	1838	73.1	4.51	4800
Epoxy resin	1.13	75	3.10	5.26	–

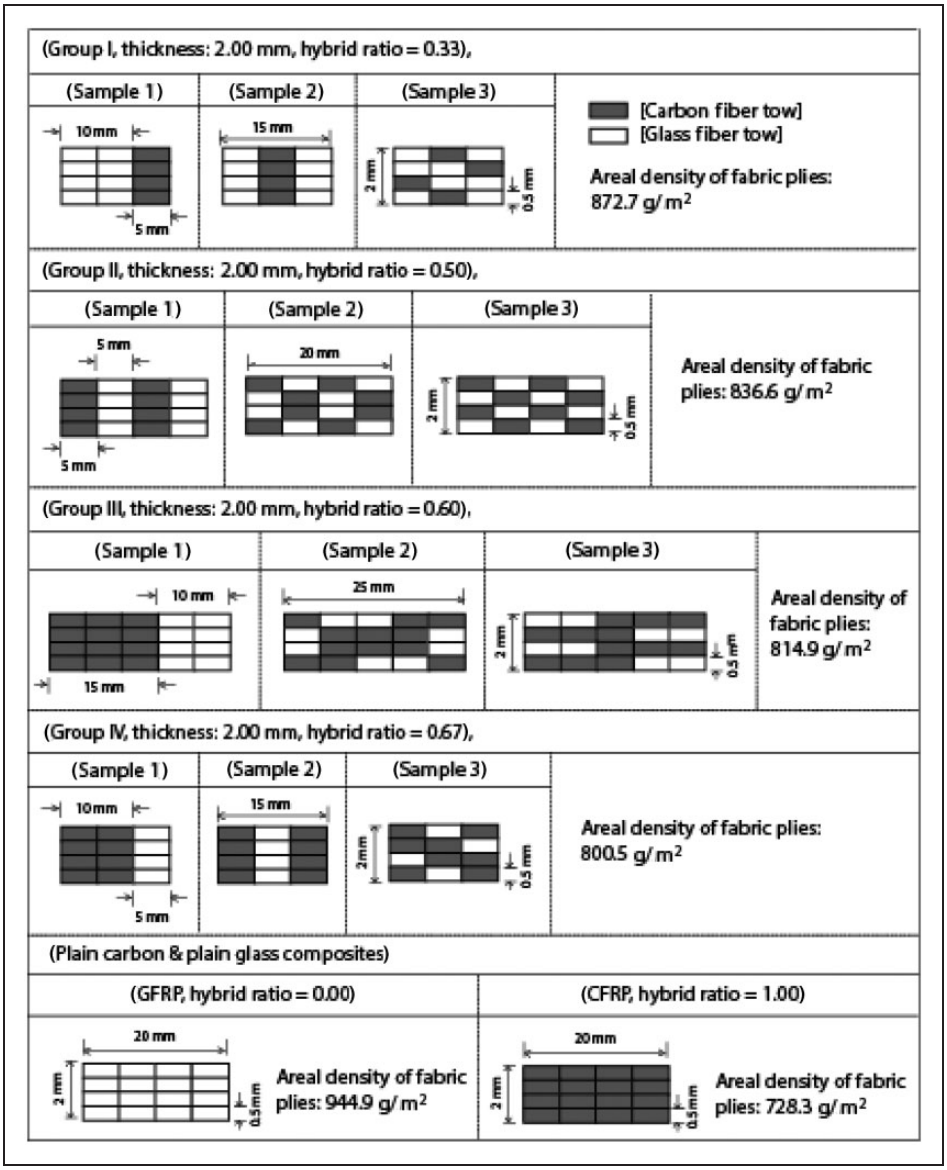

Figure 1. Laminate geometry of plain and intra-layer hybrid composites prepared for the study.

carbon and glass fiber bundle-to-bundle ratio C:G is 1:2 (5 mm:10 mm), where the composition is V_{fc},, 0.33; V_{fg}, 0.67. In group II, the carbon and glass fiber ratio C:G is 1:1 (5 mm:5 mm), where the composition is V_{fc}, 0.50; V_{fg}, 0.50. In group III the their ratio is C:G, 3:2 (15 mm:10 mm), where the composition is V_{fc}, 0.60; V_{fg}, 0.40. In group IV, the carbon and glass fiber ratio is C:G, 2:1 (10 mm:5 mm), where the composition

is V_{fc}, 0.67; V_{fg}, 0.33, where V_{fc} is the proportion of carbon fiber content and V_{fg} is the proportion of glass fiber content.

For each group, three samples were prepared with different dispersions of the glass and carbon fibers within the hybrid composites. Sample 1 in group I has a low degree of dispersion. Sample 2 has a moderate degree of dispersion, and for sample 3 the degree of dispersion is comparatively high (Figure 1). A similar strategy applies for the samples in groups II, III, and IV. Plain carbon fiber-reinforced plastics (CFRP) and plain glass fiber-reinforced plastics (GFRP) were also made to compare the properties with those of hybrid samples in groups I, II, III and IV. The hybrid ratio was introduced to characterize the degree of hybridization (''0'' for plain glass composite and ''1'' for plain carbon composite).

Composite manufacturing

Vacuum-assisted resin infusion techniques have become popular in the manufacture of composites.[40] The most popular terms to describe vacuum infusion processes are: vacuum-assisted resin transfer molding (VARTM),[41,42] vacuum-assisted resin infusion molding (VARIM),[43] Seemann composites resin infusion molding process (SCRIMP^{TM}),[44] vacuum bag resin transfer molding (VBRTM),[45] vacuum-assisted resin infusion process (VARI),[46] and so on.

All of these processes fundamentally use the same technology, and describe methods based on the impregnation of a dry reinforcement by liquid thermo-set resin driven under vacuum. VARI, with the assistance of a vacuum-bagging method, is the manufacturing technique that was applied for the manufacture of four types of laminated composites. Figure 2(a) schematically shows the vacuum bagging and resin infusion process and the photograph in Figure 2(b) was taken during the manufacture of the composites.

Plies were arranged following Figure 1 against the mold side and then a vacuum was applied to pump out the trapped air inside the assembly. Resin properly mixed with hardener was then infused to impregnate the layup. Several items were used in the vacuum bagging process as shown in Figure 2(a). During the curing process, laminates were kept at a constant pressure of 0.1 MPa and at a constant temperature of 60°C for 6 h.

Testing of composites

Tensile test

Test specimens from each of the four groups of hybrid composites were cut according to the ASTM: D3039-76 standard[47] as shown in Figure 3(a). Glass/epoxy tabs were used at each end of the specimen to avoid gripping effects (Figure 3(b)). The sample was held between the grippers of the Universal Testing Machine (UTM), Instron 550R, and extended until fracture occurred. The crosshead displacement rate was 2 mm/minute (0.034 mm/s) and the experiment was conducted at room temperature. For each sample eight tests were performed. An extensometer was used as a strain-indicating device and was attached to the surface of the test specimen in such a way that it did not cause damage to the specimen. Tensile strain was determined by averaging the surface strain indicated at each data point. After the failure of carbon fiber sections, the surface strain could not be measured further because the sample surface was damaged. In order to solve this problem, the crosshead displacement of the machine was used indirectly to calculate the strain after carbon fiber section failure. The method was accurate because the crosshead displacement is proportional to the applied load, showing only a small variation after the failure of carbon fiber sections through hybrid laminates. The tensile strength was calculated for each data point and the average ultimate tensile strength (maximum stress at which composites failed) and rupture strains (strains at maximum load) were noted (Table 2). The tensile modulus was calculated by taking the initial strains into account (from the slope between 0.1% strain to strain at the yield point). Results were also prepared for GFRP and CFRP (Table 3). Overall fiber volume fractions (V_f) and density (ρ) of the composites are presented below in Table 4. The density of each composite sample was determined using the water displacement method by measuring its weight in air and in water. The void content was measured by matrix digestion in heated concentrated sulfuric acid according to the ASTM 3171 standard test.[48] Specimens with different porosity levels ranging from 0% to 0.6% were obtained and the results averaged.

Compression test

Test specimens for compression test were cut according to the ASTM: D3410 standard[49] as shown in Figure 4(a). Glass/epoxy tabs were used at each end of the specimen to avoid gripping effects (Figure 4(b)). The specimen was held in a fixture and a compressive load was applied to produce compression. The load, 2 mm/minute (0.034 mm/s), was applied until the specimen cracked. Eight tests were carried out for each of the samples. Stress–strain plots were generated and the average ultimate compressive stress (maximum stress at which composites fail) and rupture strains (strains at maximum stress) were noted (Table 5). Compressive tests were also carried out on plain glass and plain carbon composites; the average compressive test results are presented in Table 6.

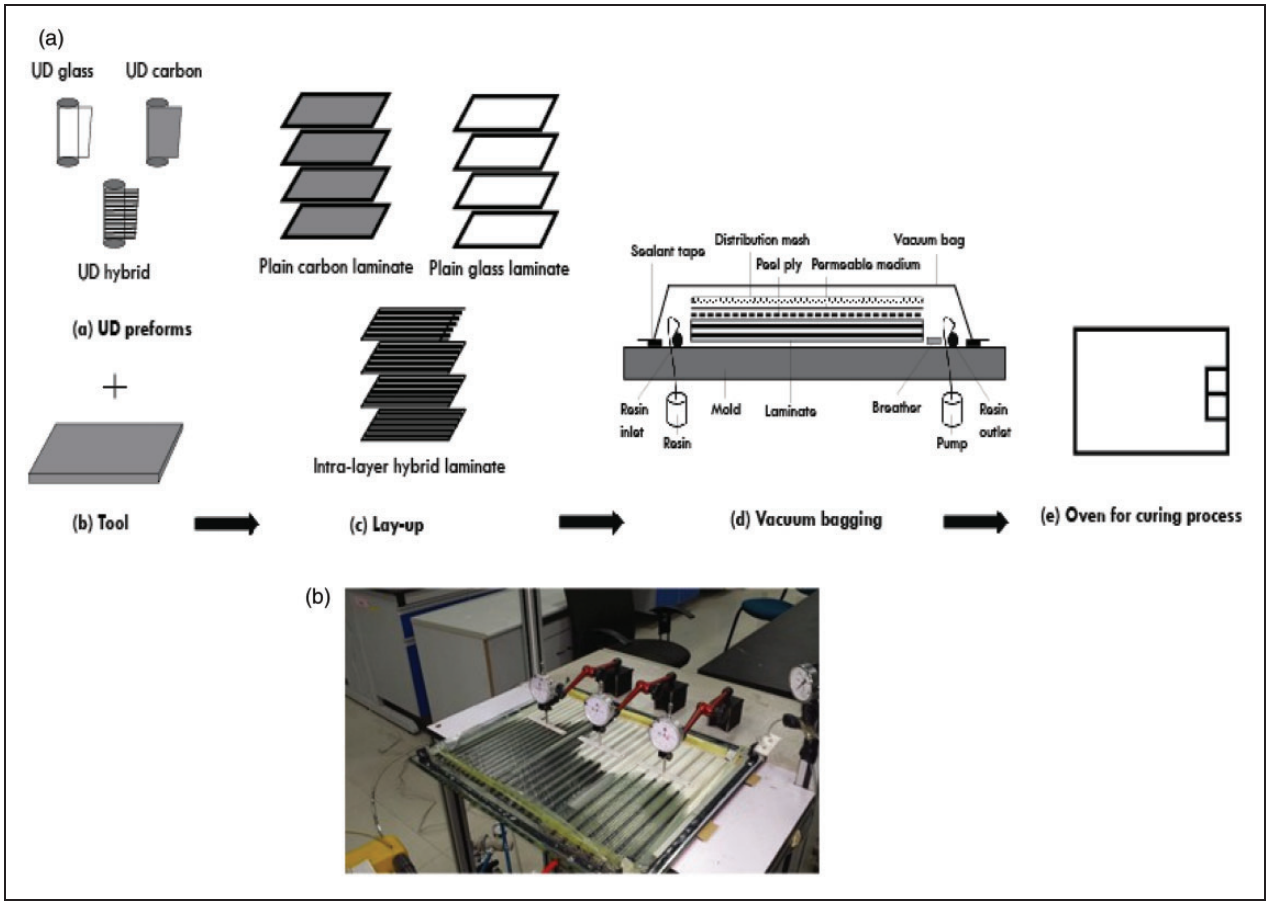

Figure 2. (a) Schematic representation of the VARI process; (b) resin infusion (photograph taken during manufacture).

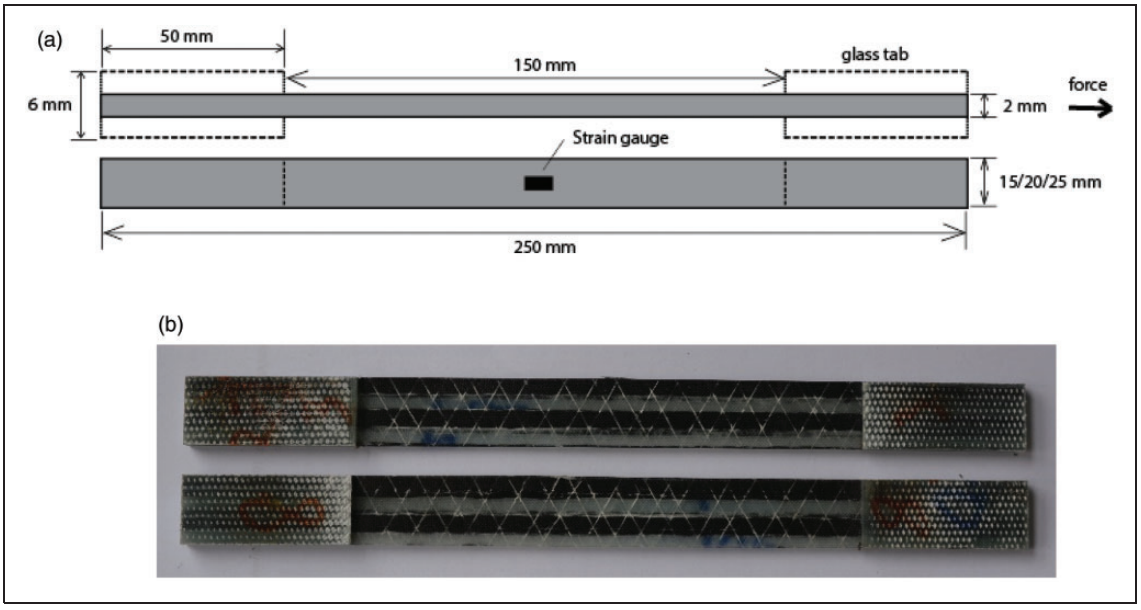

Figure 3. (a) Dimensions of the tensile test specimen (ASTM: D3039-76); (b) tensile test specimen.

Table 2. Tensile properties of the glass-carbon intra-layer hybrid composite specimens

Composite specimen	Ultimate failure strain (%)	Ultimate tensile strength (MPa)	Tensile modulus (GPa)	Specific strength (kN m/kg)	Specific stiffness (MN m/kg)
Group I					
Sample 1	2.10 (±0.04)	1025 (±20.78)	49 (±2.4)	774	37
Sample 2	2.09 (±0.05)	1045 (±15.89)	50 (±2.51)	789	38
Sample 3	2.09 (±0.09)	1105 (±18.71)	53 (±2.64)	834	40
Group II					
Sample 1	2.04 (±0.02)	1263 (±16.84)	62 (±3.00)	965	47
Sample 2	2.05 (±0.02)	1270 (±18.21)	62 (±2.63)	970	47
Sample 3	2.05 (±0.08)	1308 (±16.54)	64 (±2.99)	999	49
Group III					
Sample 1	2.02 (±0.02)	1341 (±15.98)	66 (±3.34)	1033	51
Sample 2	2.02 (±0.03)	1350 (±19.21)	67 (±3.98)	1040	51
Sample 3	2.05 (±0.02)	1368 (±14.38)	67 (±2.51)	1054	51
Group IV					
Sample 1	1.99 (±0.03)	1425 (±16.35)	72 (±4.61)	1109	56
Sample 2	2.00 (±0.03)	1452 (±17.78)	73 (±3.14)	1131	57
Sample 3	2.00 (±0.08)	1460 (±17.63)	73 (±2.66)	1137	57

Table 3. Tensile properties of plain CFRP and plain GFRP

Composite specimen	Ultimate failure strain (%)	Ultimate tensile strength (MPa)	Tensile modulus (GPa)	Specific strength (kN m/kg)	Specific stiffness (MN m/kg)
Experimental					
CFRP	1.70 (±0.02)	1785 (±21.88)	105 (±5.25)	1443	85
GFRP	2.51 (±0.03)	835 (±14.65)	33 (±1.63)	572	23
Finite element analysis					
CFRP	1.64	1857	113	1501.229	91.36
GFRP	2.60	867	33	587.030	22.83

CFRP: carbon fiber-reinforced plastics; GFRP: glass fiber-reinforced plastics.

Finite element analysis

The hybrid composites being investigated in this study were made of two types of fibers, unidirectional T620S carbon and E-glass, into a common matrix of epoxy. In this study, the tensile and compressive behaviors of hybrid composites were studied using the ABAQUS/Explicit (version 6.11) commercial software package on a Windows XP® operation system platform. Figure 5(a) and (b) show the FEA tensile and compressive test specimens, respectively. Based on the constituent properties, composite properties including the longitudinal modulus E_{11}, the transverse moduli E_{22} and E_{33}, and the shear moduli G_{12}, G_{13}, and G_{23} were derived using Hashin's model (Tables 7 to 11).[50] Hashin damage criterion was selected in the FEA models to simulate the failure and damage process of the intra-layer and inter-layer hybrid composites (Tables 12 and 13).[50] Hashin failure criteria consider that there are four modes of failure: fiber and matrix failure, under both tensile and compression stress.

Because the Hashin formulation does not consider failure by delamination, in this work a surface-to-surface cohesive model was created and the quadratic traction damage initiation criterion (with normal shear/shear-1 only/shear-2 only: 75 MPa (tensile strength of epoxy resin), linear energy type damage evolution with Benzeggagh–Kenane type mixed-mode behavior (BK exponent 1.45) and normal fracture energy, 1st shear fracture energy and 2nd shear fracture energy (calculated from the load displacement curve of epoxy resin)) for cohesive surfaces was included in the Hashin damage models (Figure 6). Traction separation description is suitable when the thickness of the interface can be considered to be zero. Surface-based

Table 4. Fiber volume fractions, proportion of the individual fiber types, and density of the composites

Composite specimen	Overall fiber volume fractions (V_f)	Proportion of fiber type		Density of composite (g/cc)
		Carbon fiber (V_{fc})	Glass fiber (V_{fg})	
GFRP	0.539	0.00	1.00	1.460
Group I				
Sample 1	0.430	0.33	0.67	1.325
Sample 2	0.429	0.33	0.67	1.324
Sample 3	0.430	0.33	0.67	1.327
Group II				
Sample 1	0.431	0.50	0.50	1.312
Sample 2	0.433	0.50	0.50	1.319
Sample 3	0.434	0.50	0.50	1.317
Group III				
Sample 1	0.441	0.60	0.40	1.285
Sample 2	0.438	0.60	0.40	1.289
Sample 3	0.444	0.60	0.40	1.285
Group IV				
Sample 1	0.458	0.67	0.33	1.271
Sample 2	0.452	0.67	0.33	1.280
Sample 3	0.455	0.67	0.33	1.277
CFRP	0.563	1.00	0.00	1.237

GFRP: glass fiber-reinforced plastics; CFRP: carbon fiber-reinforced plastics.

cohesive behavior, a simplified method, was used to model cohesive surface connections with a negligibly small interface thickness using the traction–separation constitutive model. Data input for surface-based cohesive behavior were: tangential behavior: frictionless, normal behavior with linear pressure-over closure; cohesive behavior: only slave nodes initially in contact.

ABAQUS/Explicit analysis used the three-dimensional deformable solid, extrusion type. The materials' properties input to the FEA calculation were the density, mechanical properties, and the damage criteria. The density of the tube composite was calculated from the constituent densities. The rectangular model was extended in the *x*-direction as shown in Figure 5(a) and (b). Velocity of the reference point was set at 0.0334 mm/s to mimic the experimental loading condition of 2 mm/minute loading. An Encastre boundary condition was applied to one side of the rectangular model, as shown in Figure 5(a) and (b). This was to ensure no movement and no rotation in any direction at this end of the model. Y-axis of the model was applied with y-symmetry (Y-SYMM). The meshed hybrid composite rectangular model is shown in Figure 5(a) and (b). Meshing of the model was done with the eight-node reduced integration element (C3D8R). The number of meshes used was 6000 for tensile test specimens and 1600 for compressive test specimens.

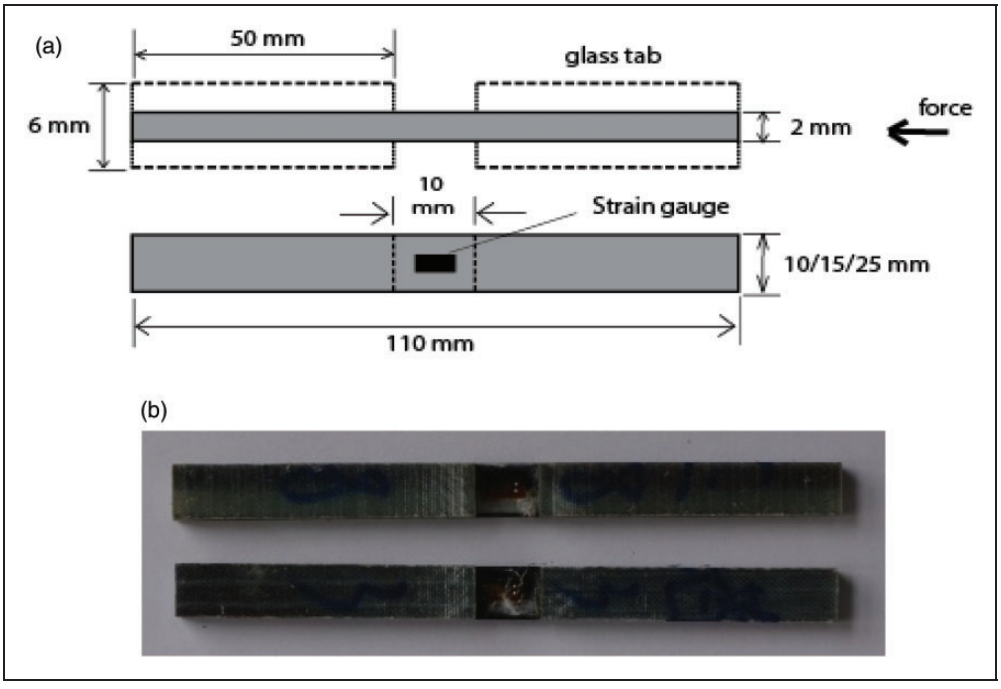

Figure 4. (a) Dimensions of the compressive test specimen (ASTM: D3410); (b) compressive test specimen.

Table 5. Compressive properties of the glass–carbon intra-layer hybrid composite specimens

Composite specimen	Ultimate failure strain (%)	Ultimate compressive strength (MPa)	Compressive modulus (GPa)	Specific strength (kN m/kg)	Specific stiffness (MN m/kg)
Group I					
Sample 1	1.26 (±0.05)	465 (±11.01)	37 (±2.83)	351.344	27.87
Sample 2	1.26 (±0.02)	471 (±10.87)	37 (±3.03)	355.982	28.24
Sample 3	1.28 (±0.03)	484 (±8.89)	38 (±2.89)	365.542	28.53
Group II					
Sample 1	0.97 (±0.03)	561 (±14.74)	58 (±1.51)	428.343	44.15
Sample 2	0.97 (±0.04)	568 (±12.39)	59 (±2.61)	434.189	44.75
Sample 3	0.98 (±0.02)	580 (±13.21)	59 (±2.73)	442.822	45.18
Group III					
Sample 1	0.92 (±0.04)	615 (±15.41)	67 (±3.03)	473.960	51.51
Sample 2	0.93 (±0.04)	636 (±17.32)	68 (±3.53)	489.905	52.67
Sample 3	0.95 (±0.05)	650 (±13.40)	68 (±3.33)	500.718	52.70
Group IV					
Sample 1	0.87 (±0.02)	688 (±12.89)	79 (±4.22)	535.426	61.54
Sample 2	0.87 (±0.02)	709 (±17.67)	81 (±3.88)	551.480	63.38
Sample 3	0.89 (±0.03)	726 (±18.97)	82 (±4.05)	564.571	63.43

Table 6. Compressive properties of the plain carbon and plain glass fiber-reinforced composites

Composite specimen	Ultimate failure strain (%)	Ultimate compressive strength (MPa)	Compressive modulus (GPa)	Specific strength (kN m/kg)	Specific stiffness (MN m/kg)
Experimental					
CFRP	0.7 (±0.07)	1081 (±12.33)	154 (±5.87)	874	125
GFRP	1.51 (±0.03)	489.7 (±8.48)	32 (±2.66)	335	22
Finite element analysis					
CFRP	0.65	1126	173	910.320	140.04
GFRP	1.52	519	34	355.229	23.36

CFRP: carbon fiber-reinforced plastics; GFRP: glass fiber-reinforced plastics.

Results and discussion

Tensile properties

Tensile strength and tensile modulus. Among all the composite laminates, CFRP has the maximum compressive stress, minimum failure strain, and hence the maximum compressive modulus. The opposite is true for GFRP (Table 3). For brittle properties, the curves show the lowest displacement among all the tested structures. In the case of sample 3 in groups I and III, it is seen that after cracking the structure did not tend to show any plateau region whatsoever and directly reached a critical point in carrying a high load/stress, which led to catastrophic failure. This is also true for plain CFRP. Sample 3 under Group II and Group IV showed linearity and ductility (Figure 7(a)). These hybrid structures to some degree tend to show some ductility because of having a highly dispersed mixture of brittle carbon fiber and ductile glass fiber within their structures. However, in terms of final failure it is observed that they also failed catastrophically. Figure 7(a) shows the stress–strain plots of the intra-layer hybrid specimens (sample 3 in groups I, II, III and IV) and Figure 7(c) shows the stress–strain plots of specimens in group II. In Figure 7(c), it is evident that sample 3 has some sort of plateau region near the end of the curve, whereby the composite has failed in a more controlled manner than the other two samples in the same group, though the final failure is catastrophic.

Figure 7(b) and (d) show the experimental results of these composites against FEA results. In general, the results are in good agreement (the tensile finite element (FE) stress contour is shown below in Figure 16). Although FEA slightly overestimated the stress, the

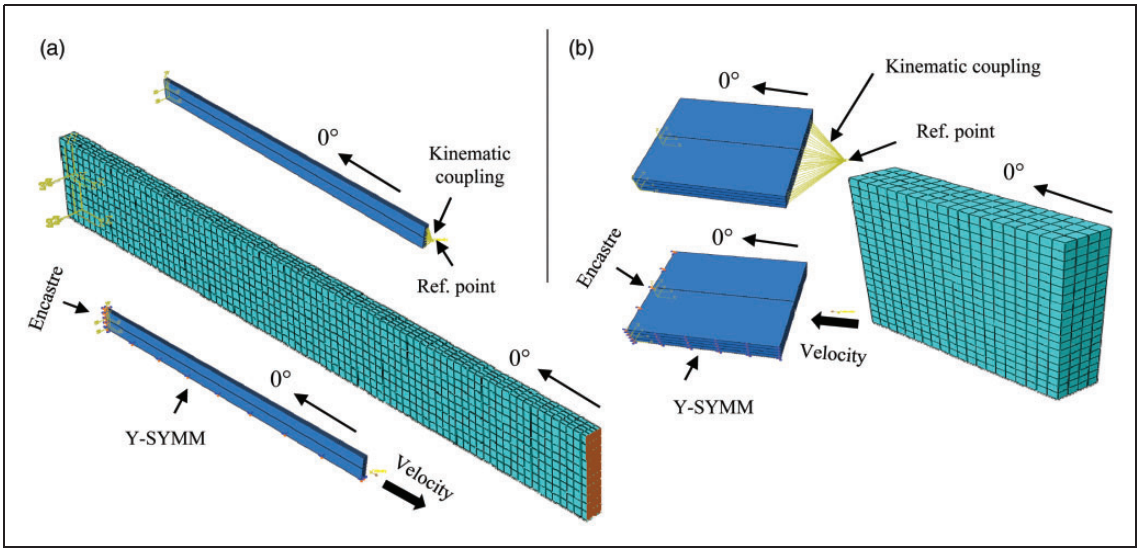

Figure 5. Load, boundary condition, and meshing in FEA. (a) Tensile test; (b) compression test.

Table 7. Density of the composites for finite element analysis input

Material	ρ (g/cc)
CFRP	1.237
GFRP	1.460

CFRP: carbon fiber-reinforced plastics; GFRP: glass fiber-reinforced plastics.

Table 8. Young's modulus in fiber, for transverse and normal directions of the composite materials for finite element analysis input

Material	E11 (GPa)	E22 (GPa)	E33 (GPa)
CFRP	105.01	9.4	9.4
GFRP	33.26	16.2	16.2

CFRP: carbon fiber-reinforced plastics; GFRP: glass fiber-reinforced plastics.

Table 9. Poisson's ratio in three directions for finite element analysis input

Material	Nu_{12}	Nu_{13}	Nu_{23}
CFRP	0.0209	0.0209	0.33
GFRP	0.0278	0.0278	0.40

CFRP: carbon fiber-reinforced plastics; GFRP: glass fiber-reinforced plastics.

Table 10. Shear modulus in three directions for finite element analysis input

Material	G_{12} (GPa)	G_{13} (GPa)	G_{23} (GPa)
CFRP	4.5	4.5	6.25
GFRP	5.83	5.83	11.34

CFRP: carbon fiber-reinforced plastics; GFRP: glass fiber-reinforced plastics.

trends are in good agreement. The reason for this overestimation could be due to FEA always considering ideal testing conditions, meaning that there are no experimental errors in FEA. Besides, the three-dimensional deformable parts taken in FEA have perfectly homogenous properties that, in practice, is not possible. This is because there could be some flaws present in the experimental specimens. Since FEA always considers ideal testing conditions and no flaws in the specimen, the results obtained are always higher than those obtained from experiments.

From Table 2 it is clear that in each group (when the overall volume fraction is same for all and the proportions of the two fiber types are constant), the performance of sample 3 is better than that of the two other samples. This signifies that the ultimate tensile stress improves with an increase in the dispersion of the two fiber types within the hybrid systems. Carbon fiber parts become sandwiched between glass fiber parts when the dispersion improves and the evolution of possible damage in carbon fiber is constrained by the surrounding glass fibers, thereby resulting in improved performance. The effect of dispersion on tensile stress is neither that large nor uniform; an erratic effect has

Table 11. Tensile and compressive strength in fiber, for transverse and normal directions, and transverse shear strength for finite element analysis input

Material	X_T (MPa)	X_C (MPa)	Y_T (MPa)	Y_C (MPa)	Z_T (MPa)	Y_S (MPa)
CFRP	1785.3	1080.5	74	237	120	64
GFRP	835	489.7	60	140	65	35

CFRP: carbon fiber-reinforced plastics; GFRP: glass fiber-reinforced plastics.
X_T, Y_T and Z_T are the tensile strength in fiber, transverse and normal directions, respectively.
X_C and Y_C are the compressive strength in fiber and transverse directions, respectively.
Y_S is the shear strength in transverse direction.

Table 12. Hashin damage strength parameters input in finite element analysis

	Properties					
Composite	X_T (MPa)	X_C (MPa)	Y_T (MPa)	Y_C (MPa)	X_S (MPa)	Y_S (MPa)
CFRP	1785.3	1080.5	74	237	120	65
GFRP	835	489.7	60	140	65	35

X_S is the shear stress in fiber direction.

Table 13. Hashin damage evolution parameters input in FEA

	Properties			
Composite	Tensile fracture energy (*x*-direction)	Compressive. fracture energy (*x*-direction)	Tensile fracture energy (*y*-direction)	Compressive fracture energy (*y*-direction)
CFRP	1517.5	1416	52.54	465.9
GFRP	1047.95	972.2	90.6	311.4

CFRP: carbon fiber-reinforced plastics; GFRP: glass fiber-reinforced plastics.

been observed. In particular, sample 3 in group I has an ultimate tensile strength of 1105.297 MPa, which is 1.05 times that of sample 2 and 1.07 times that of sample 1. Samples in groups II, III, and IV show, to some extent, similar erratic trends. For the samples in group III, it is seen that the effect is not very significant. This is due to having very high carbon fiber and glass fiber tow thicknesses. The tow thickness of the carbon fiber and glass fiber parts being high, it is not possible to have a better dispersion when compared to the specimens in other groups. In terms of the effect of dispersions of the two fiber types on ultimate tensile strength, the hierarchy is: sample 3 > sample 2 > sample 1. Due to the overwhelming amount of experimental data confirming the importance of dispersion, this is undoubtedly one of the most critical parameters that influence mechanical properties.[6,34,36–38] Fukunaga et al.[39] proved that hybrid effect for failure strain increases when the bundle size decreases from four fibers to a single fiber. Though the authors did not clarify how large the increase was, but through analyzing their figures an enhancement in the strength by about 10% can be estimated. An increase in strength of about 10% can be estimated. Zhang et al.[21] reported that the ultimate tensile strength of unidirectional glass/flax composites increased by 15% when dispersion was improved.[21] Apart from the strength issue, Mishnaevsky and Dai[51] showed that finer dispersion leads to slower development of internal damage. To understand the effect of dispersion, a smaller bundle size would perhaps be better.

Sample 3 in group IV has an ultimate tensile strength of 1460.687 MPa, which is 6.72% higher than that of sample 3 in group III, 11.64% higher than that of sample 3 in group III, and 32.15% higher than that of sample 3 in group I. This implies that the ultimate tensile strength of the composite improves with an increase of the proportion of carbon fibers, which can also be seen in Figure 7(b). This means that the percentage volume fraction/proportion of carbon fibers in the glass–carbon mixing ratio plays a significant role in determining the tensile strength of the hybrids, as there is a strength compatibility of carbon fiber throughout the hybrids. The tensile strengths of other

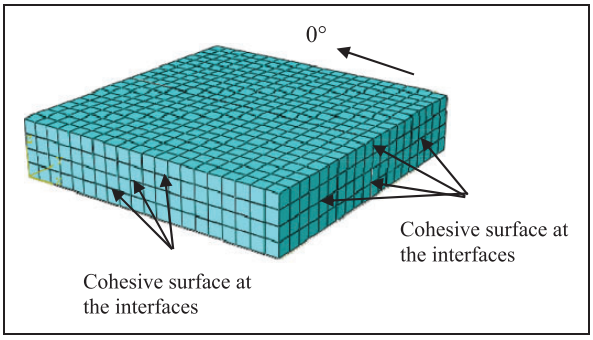

Figure 6. Cohesive surface modeling at the interfaces in finite element analysis.

samples in different groups are presented in Table 2. A similar trend of effects is noticed. In terms of the effect of percentage volume fraction/proportion of the carbon fiber on tensile strength, the hierarchy of different groups can be presented as: group IV > group III > group II > group I.

Sample 3 in group IV, with the maximum carbon fiber content, exhibited the maximum tensile strength compared to all other samples in other groups. The dispersion of the two fiber types is also high for sample 3 when compared to samples 1 and 2 in the same group. Dispersions of the two fiber types and composition of the hybrid specimens also influenced the tensile modulus (Table 2, Figure 8). The variation of tensile modulus shows a uniform increase with the increase in the proportion of carbon fibers.

Results were also generated for plain CFRP and plain GFRP composite laminates (Table 3). When compared to the ultimate tensile strength of CFRP, a percentage loss in ultimate tensile strength is observed for all hybrid specimens in every group. Percentage losses in tensile strength of 42.56%, 41.42%, and 38.08% were noticed for samples 1, 2, and 3 in group I when compared to that of CFRP. This shows that dispersion of the two fiber types has an effect on the percentage loss in tensile strength. As the dispersion improves, the loss in tensile strength decreases.

For sample 1 in group I, the percentage loss in tensile strength is 42.56%, for sample 1 in group II it is 29.24%, for sample 1 in group III it is 24.86%, and for sample 1 in group IV it is 20.16%. It is seen that the percentage loss in tensile strength decreases as the proportion of carbon fibers increases. Percentage loss in tensile modulus is also noticed when compared to that of CFRP. Pandya et al.[16] reported a loss of tensile strength for hybrids when compared to a plain carbon composite. Two types of inter-layer hybrids were made, H1 $[G_3C_2]_s$ and H2 $[C_2G_3]_s$, composed of 8 H satin plain carbon T300 fabric and E-glass, for the analysis. A loss of 17.2% and 21.37% in tensile strength was reported for H1 and H2, respectively.[16]

Tensile failure strain. Dispersion of the two fiber types did not influence the tensile failure strains significantly, yet higher values were noted for the high dispersion specimens (sample 3) in each group. The highest tensile failure strain was noted for the samples in group I, where the proportion of carbon fibers was the lowest (just 0.33). The tensile failure strain definitely improves with incorporation of the high-elongation glass fibers, but no clear trend is associated with varying proportions of glass and carbon fibers.

In general, a percentage increase in ultimate tensile failure strain was noticed for all hybrid specimens in each group when compared to that of CFRP. For sample 1 in group I, the ultimate tensile failure strain was 2.10%, therefore a 23.52% percentage increase in tensile failure strain was noticed when compared to that of CFRP. The percentage enhancement decreases as the proportion of carbon fiber content increases (see Figure 12(a) to (c) below). The rate of decrease is erratic.

In terms of the effect of dispersion on percentage tensile failure strain, the effect is not very significant (Tables 2 and 3). Percentage gain in tensile failure strain has been reported by Pandya et al.[16]. A gain of 90.4% in ultimate tensile failure strain was reported for hybrid composite H1 $[G_3C_2]_s$ when compared to plain carbon [8H satin fabric] reinforced in epoxy matrix.[16] Zhang et al.[17] hybridized woven glass and carbon fiber and found improvements in failure strain, ranging between 10% and 31%. The failure of the carbon fiber layers coincided with final failure of the hybrid composite, and no further load carrying by the glass fiber layers was observed.

Specific strength and specific stiffness. Figure 9 presents the specific strength of composites obtained from FEA and experimental tests versus the hybrid ratio. As expected, CFRP had the highest strength and GFRP had the lowest specific strength. The specific strengths of all hybrid specimens were in between those of CFRP and GFRP. With the variation of composition, the density for the hybrid composites varied as shown in Table 4. Specific strength was calculated by dividing the ultimate tensile strength by the corresponding density of the composites. The proportion of carbon fibers and dispersion of the two fiber types were both shown to have an influence on specific strength (Table 2, Figure 9). FE models slightly overestimated the specific strength.

Figure 10 presents the specific stiffness of composites obtained from FEA and experimental tests under quasi-static tensile loading versus the hybrid ratio. Specific stiffness (MN m/kg) was obtained by dividing the tensile modulus by the corresponding density of the composite specimens. As expected, CFRP had the maximum specific stiffness, followed by the hybrid

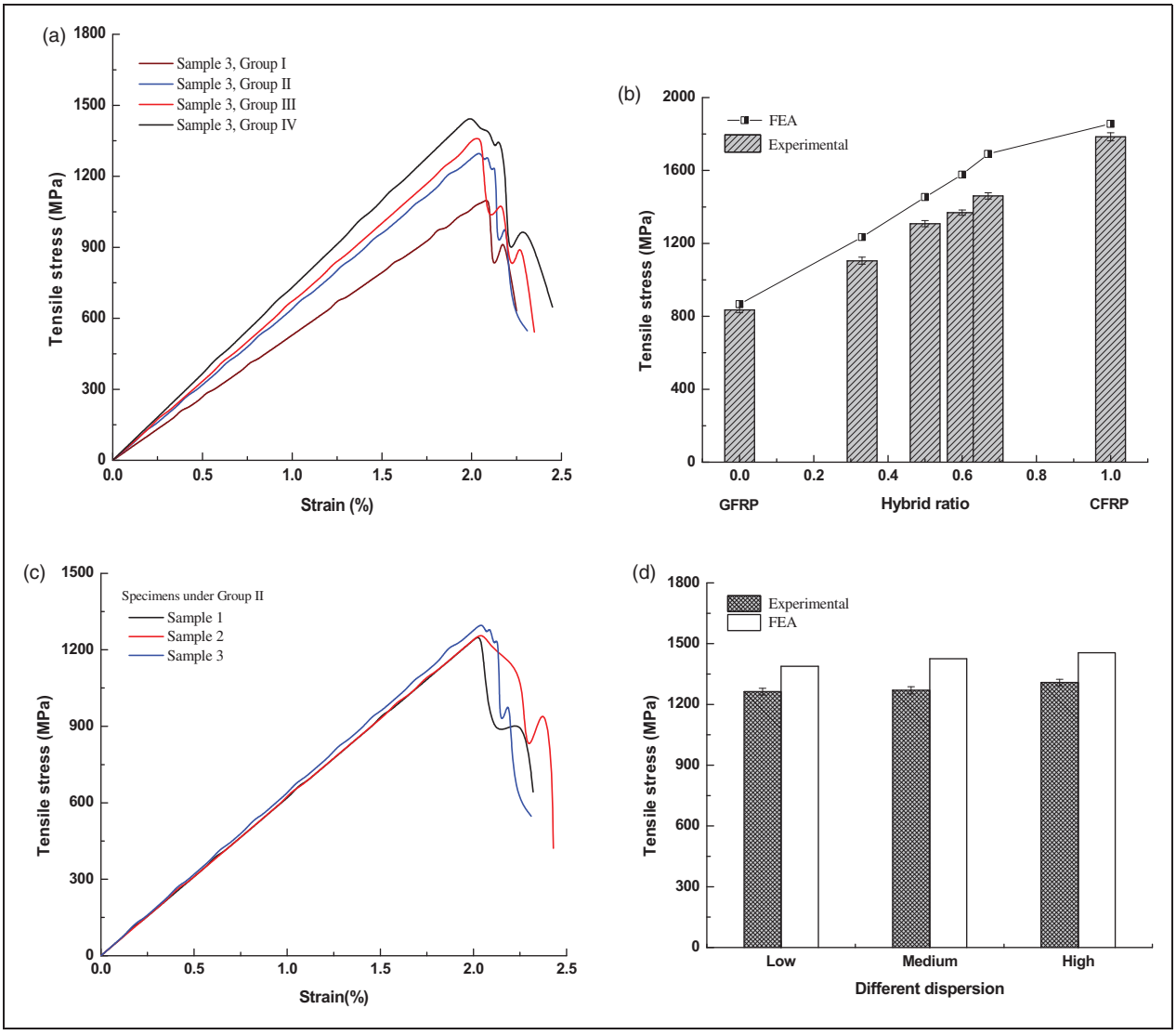

Figure 7. (a) Tensile stress-strain plots of Sample 3 under all four groups obtained experimentally (b) Maximum tensile strengths of plain laminates and Sample 3 under all four groups obtained experimentally and from FEA (c) Stressstrain plots of three composite laminates under Group II obtained experimentally (d) Maximum strengths of three composite specimens under Group II obtained experimentally and from FEA.

composites, and then GFRP. In general, the results obtained from FEA and experiments are in good agreement. It was observed that both the dispersions of the two fiber types and the composition of the hybrids were shown to have an influence on specific stiffness (Table 2 and Figure 10(a) to (c)). FE models to some extent overestimated the specific stiffness.

Hybrid effect. The expected tensile modulus of the hybrid composites can be calculated using an RoM approach. It was seen that the tensile modulus obtained from the experimental tests did not follow the RoM due to the hybridization effect. RoM is given by equation (1)[32,52]

$$E_H = (E_C \times V_C) + (E_G \times (1 - V_C)) \quad (1)$$

where E_H is the tensile modulus of the hybrid according to RoM, E_C is the modulus of plain CFRP, and E_G is the modulus of the plain GFRP. V_C is the volume fraction of CFRP in the mixing ratio, and $V_G = (1 - V_C)$. The tensile stress of hybrids (σ_H) can also be assumed in a similar way, as in equation (2)

$$\sigma_H = (E_C \times \varepsilon_C \times V_C) + (E_G \times \varepsilon_G \times (1 - V_C)) \quad (2)$$

where ε_C and ε_G are the tensile strains of plain carbon and plain glass composites, respectively.

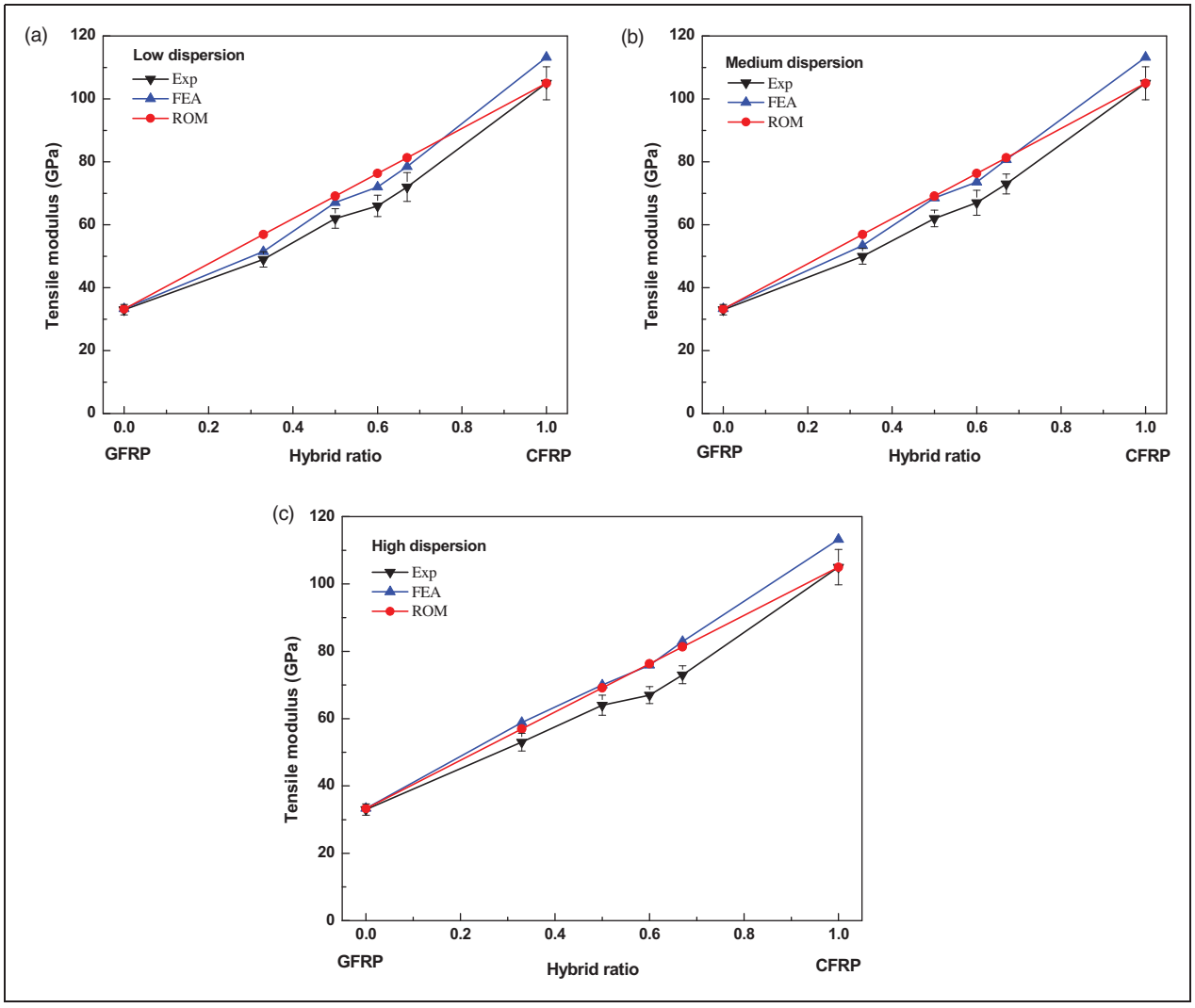

Figure 8. Tensile modulus of composites versus hybrid ratio. (a) Low dispersion; (b) medium dispersion; (c) high dispersion.

The hybrid effect is defined as the positive or negative deviation of a certain property from that obtained using RoM.[12,53,54] The hybrid effect is given by equation (3), where λ_H is the hybrid effect usually calculated as a percentage, σ_T is the tensile strength obtained from the experimental test, and σ_H is the tensile strength obtained using RoM

$$\lambda_H = \left[\frac{\sigma_T}{\sigma_H} - 1\right] \quad (3)$$

Since none of the samples' test results followed the RoM, negative hybrid effects on ultimate tensile strength existed for all hybrid composites. Figure 11(a) to (c) plot the test results and results obtained from the RoM versus hybrid ratio. Negative hybrid effects of −10.72%, −8.96%, and −3.77% were found to exist for samples 1, 2, and 3 in group I. This dictated that dispersions of the two fiber types had an effect on the hybrid effect for tensile strength (Figure 11(d)). As the dispersion improves, the hybrid effect for tensile strength decreases. Sample 1 in group II had a negative hybrid effect of −3.57% on tensile strength. Sample 1 in group III had an effect of 4.54% and that of −3.15% for sample 1 in group IV. This dictates that, as the proportion of carbon fibers increases, the hybrid effect for tensile strength decreases.

Therefore, it was seen that both the dispersion of the two fiber types and the proportion of carbon fiber influenced the so-called hybrid effect on tensile strength (Figure 11(d)). Since the mechanical properties of carbon and glass fibers and the interface properties between fibers and matrix differ significantly, the hybridization effects also would vary for the hybrid composites.[55–57] A comprehensive review on the mechanical properties of glass/carbon hybrid composites[8] showed that the longitudinal tensile moduli are generally in

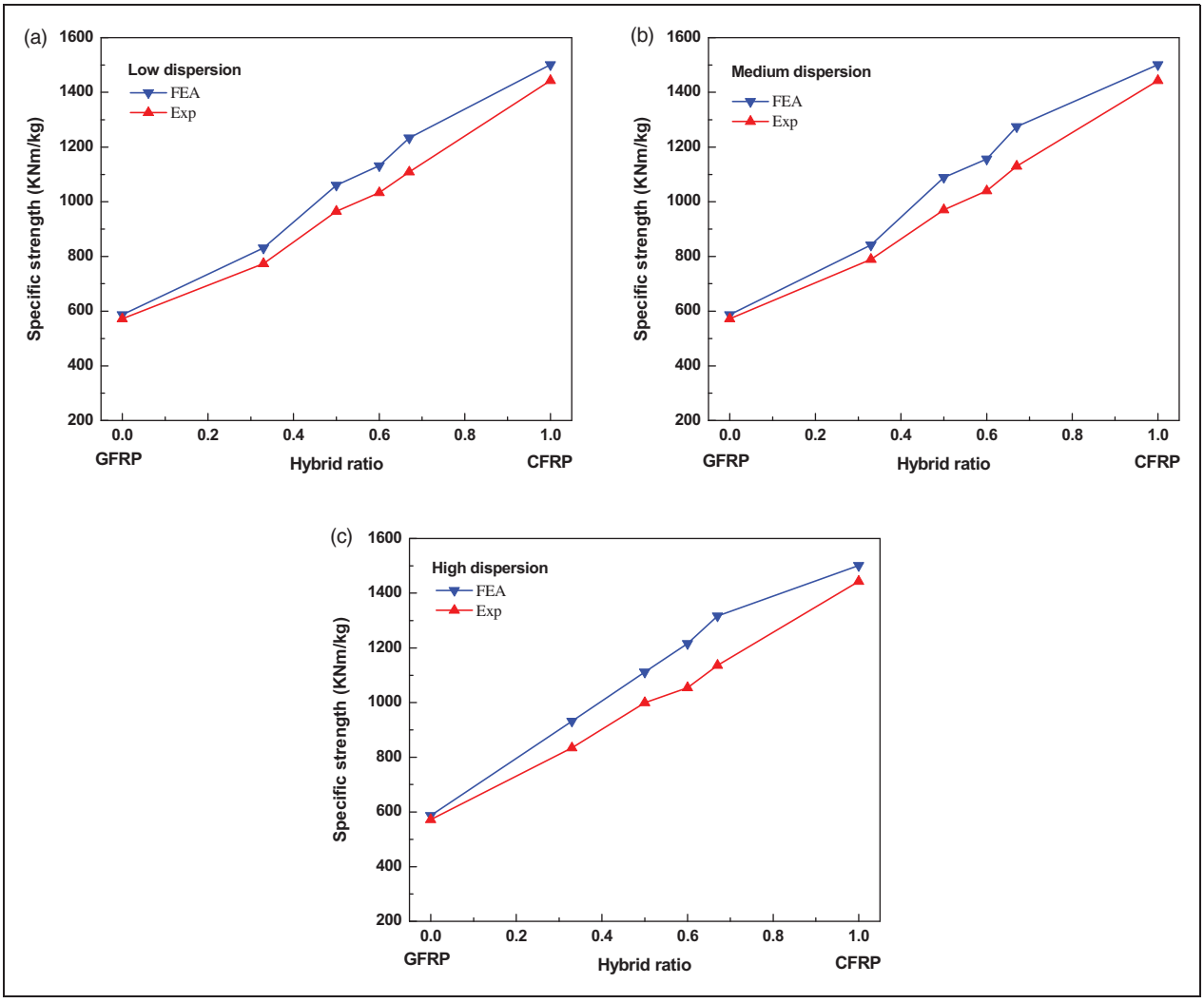

Figure 9. Specific strength (kN m/kg) of composites versus hybrid ratio. (a) Low dispersion; (b) medium dispersion; (c) high dispersion.

good agreement with the RoM, since there is a strain compatibility through the thickness of a hybrid material. By prediction based on displacement-controlled tests where iso-strain is assumed for both low elongation and HE fibers, many authors have reported that tensile strength depends on a bilinear RoM.[6,8,22,58] Ren et al.[34] observed a negative hybrid effect for a carbon/carbon hybrid composite.

The hybrid effect was also calculated for tensile failure strain. Samples in groups I and II were shown to have negative hybrid effects for ultimate tensile failure strain (Figure 12(d)). On the other hand, specimens numbered as samples 1 and 2 in group III followed the RoM (no hybrid effect).

Sample 3 in group III and all three specimens in group IV were inclined to have positive hybrid effects for ultimate tensile failure strain. Sample 3 in group III had a positive hybrid effect of +1.48% for failure strain. In group IV, positive hybrid effects on tensile failure strain were +1.53%, +2.04%, and +2.04% for samples 1, 2, and 3, respectively. Figure 12(d) shows the hybrid effect for tensile failure strain for three dispersions against hybrid ratio. Some authors have claimed that the hybrid effect for failure strain increases with increased dispersion, but they changed the relative volume fractions of both of the fiber types.[7,59,60] In this experiment, the effect of dispersion on hybrid effect for tensile failure strain, by keeping the relative volume fractions of the two fiber types the same, has been analyzed. As can be seen from the plots (Figure 12(d)) the effect of dispersion on hybrid effect for tensile failure strain is not significant. In terms of the effect of carbon fiber proportion on hybrid effect for tensile failure strain it is seen that, as the proportion increases, the hybrid effect decreases.

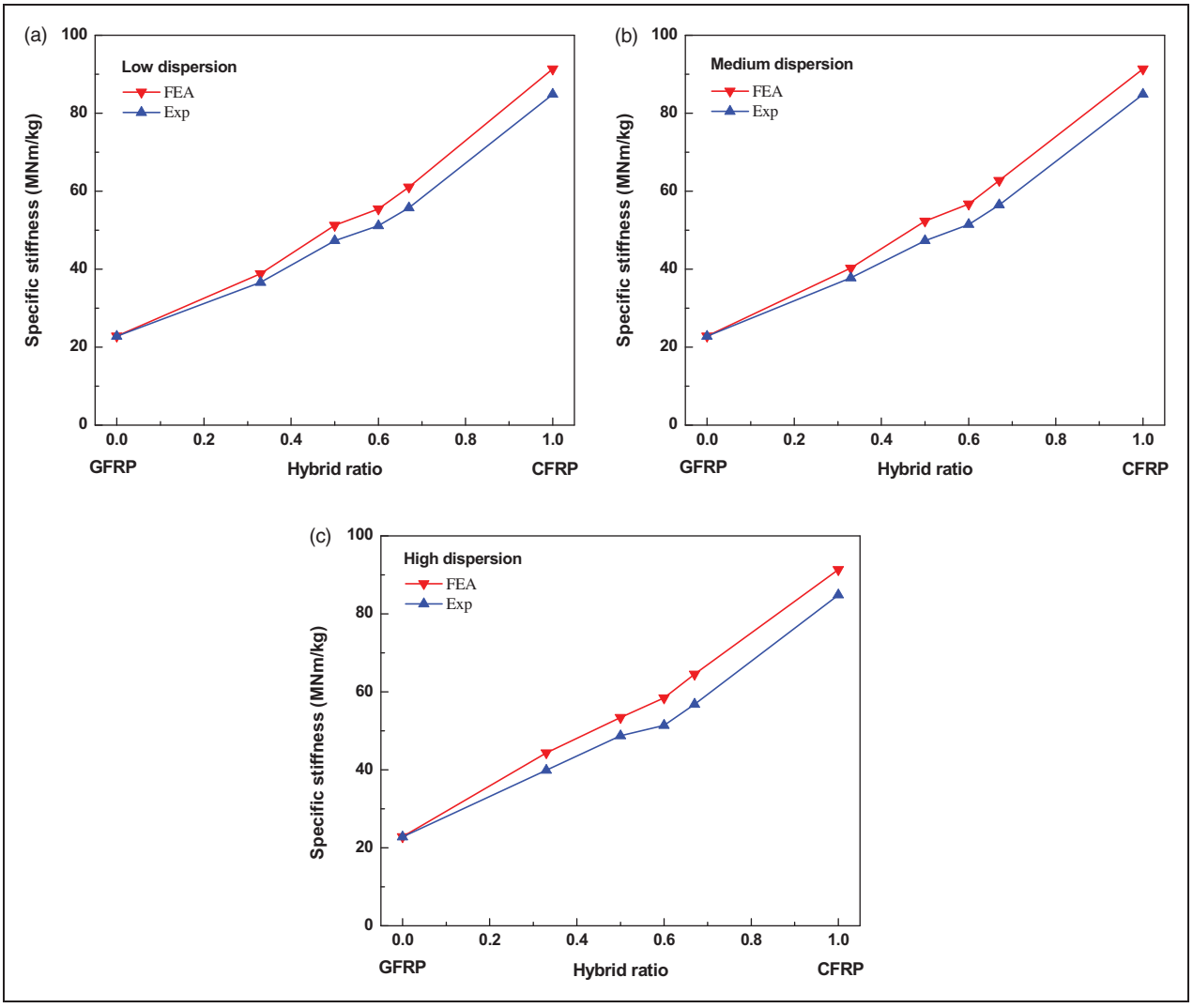

Figure 10. Specific stiffness of composites versus hybrid ratio. (a) Low dispersion; (b) medium dispersion; (c) high dispersion.

Compressive properties

Compressive strength and modulus. From Figure 13(a) to (c), it is understood that, the compression test results for specimens in group IV are higher than the other specimens in groups I, II, and III. This indicates that the compressive properties of the composite increase with increase in the proportion of carbon fibers into the compositions of hybrids. In any group and among different samples, it is seen that sample 3 had the better compressive performance which dictates that. As the dispersion improves, the compressive properties increase. The compressive stresses obtained from FEA tests (compressive FE stress contour is shown in Figure 17) and experiments are in good agreement.

In particular, sample 3 in group IV exhibited the compressive strength of 725.475 MPa, which was 1.11 times that of sample 3 in group III, 1.25 times that of sample 3 in group II, and 1.49 times that of sample 3 in group I. This signifies that, as the proportion of carbon fibers into the glass–carbon mixing ratio increases, the compressive strength increases. For other samples a similar trend is observed (Table 5). For sample 3 in group II the compressive strength was 579.654 MPa, which was 1.01 times that of sample 2 and 1.03 times that of sample 1. The effect was not that much, though a slightly better compressive strength was observed when the dispersion of the two fiber types improved (Table 5).

Results were also generated for CFRP and GFRP (Table 6). The compressive strength of CFRP was much higher than that of GFRP primarily owing to the higher stiffness of the carbon fibers and also because of the better fiber–matrix bond. A percentage loss in compressive strength for all hybrid composites was observed when compared to that of CFRP. The

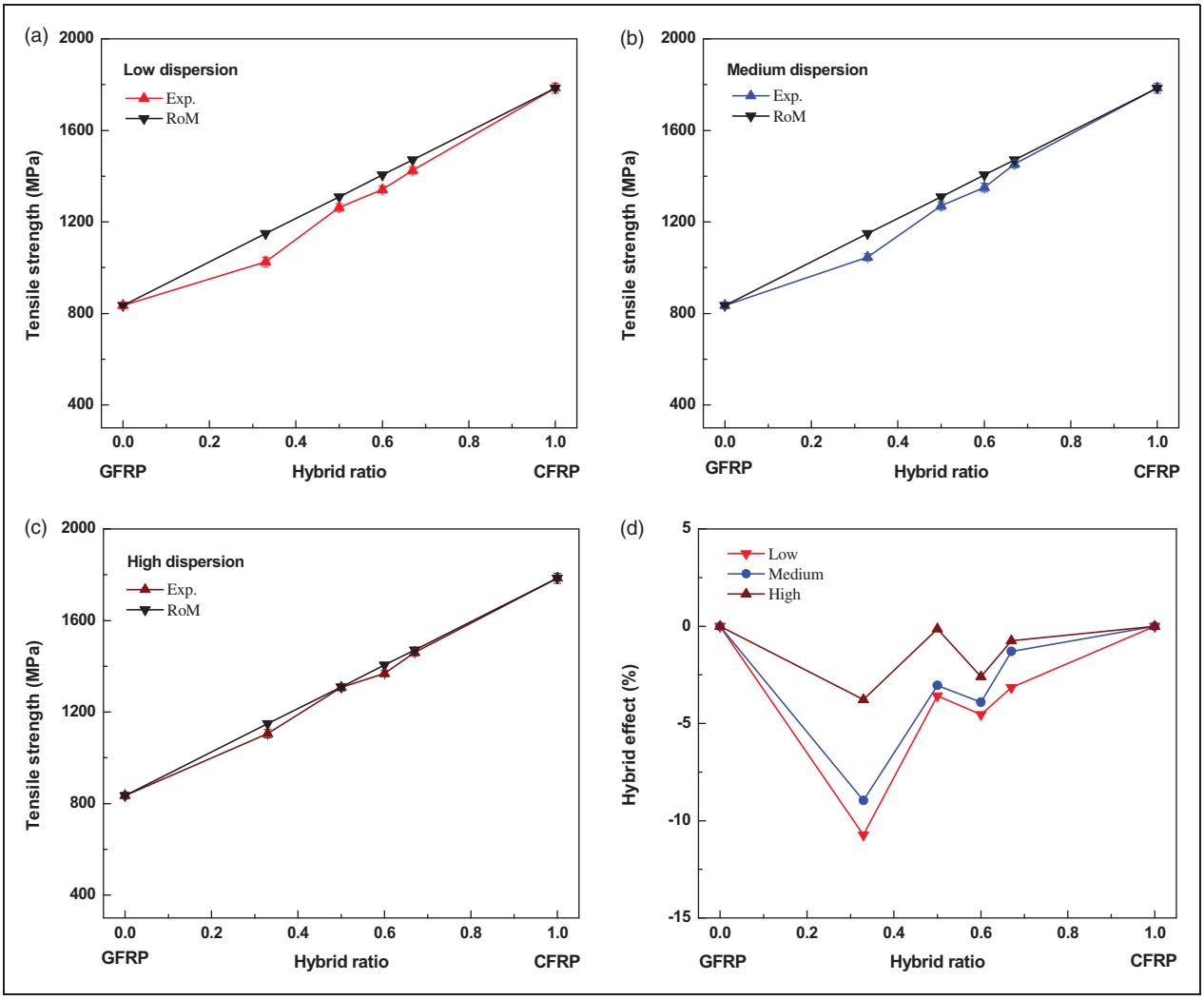

Figure 11. Test tensile strengths versus hybrid ratio: (a) low dispersion; (b) medium dispersion; (c) high dispersion. (d) Hybrid effect on tensile strength versus hybrid ratio.

percentage loss in compressive strength decreased as the carbon fiber content in the mixing ratio increased and vice versa. The dispersion further aided the performance to be much better. Similar effects were seen for the compressive modulus (Tables 5 and 6). Pandya et al.[16] reported that reduction in compressive strength for hybrid composites is not significant compared with that of 8 H satin T300 carbon/epoxy. From this data, it is seen that hybrid composites H1 $[G_3C_2]_s$ and H2 $[C_2G_3]_s$ lose 5.21% and 7.07% in compressive strength, respectively, when compared to that of plain carbon epoxy composite.[16]

Compressive failure strains. Similar types of effects were also noticed on the ultimate compressive failure strains and the percentage enhancement in compressive failure strains. Both the dispersion of the two fiber types and the composition of the hybrid specimens claimed to have an influence on compressive failure strains and strain enhancement (Figure 14(a) to (c)). As the proportion of carbon fiber increased, the compressive failure strain decreased. The effect of dispersion of fiber types on compressive failure strain was not found to be very significant. Since the proportion of carbon fibers affected the compressive failure strain, it affected the compressive modulus either as the initial strain is used to determine the modulus (initial elastic behavior) (Tables 5 and 6). From the data table reported by Pandya et al.[16] it is seen that gain in compressive failure strain for hybrid composites is not very significant. Hybrid composite H1 $[G_3C_2]_s$ gains only 2.23% and H2 $[C_2G_3]_s$ gains 5.07% in ultimate compressive failure strains when compared to that of a plain carbon/epoxy system.[16]

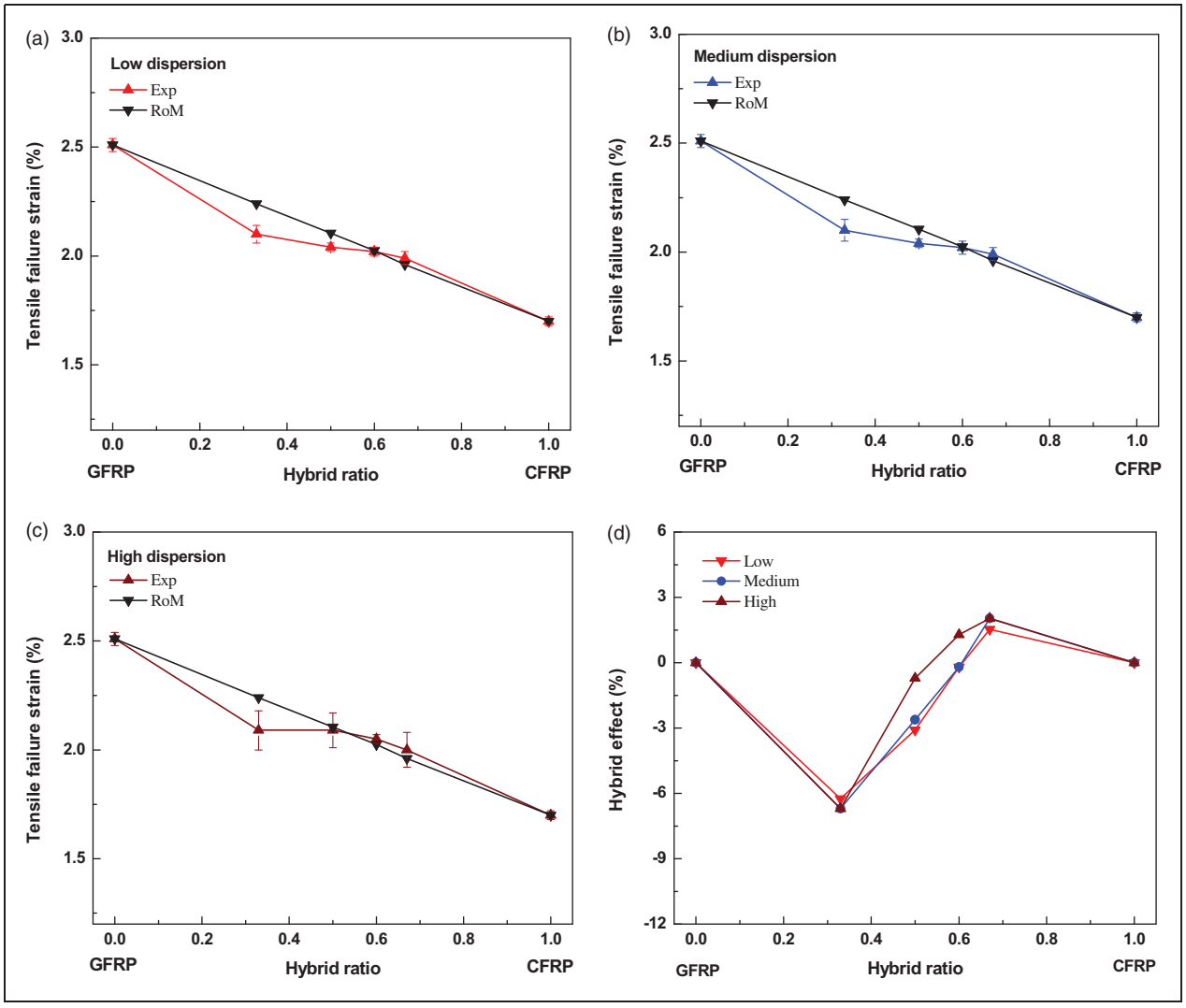

Figure 12. Tensile failure strains versus hybrid ratio: (a) low dispersion; (b) medium dispersion; (c) high dispersion. (d) Hybrid effect on failure strain versus hybrid ratio.

Specific strength and specific stiffness. Specific strength under compressive loading was achieved simply by dividing the ultimate compressive strength by the corresponding density of the composites, as shown in Tables 5 and 6. As expected, carbon fiber composite had the highest specific strength, followed by hybrids, and then glass fiber composite. Specific stiffness was also calculated for all of the composite specimens. Specific stiffness, obtained by dividing the modulus by the density, was calculated to find out the stiffness-to-weight ratio that determines which material produces structures with minimum weight. The dispersion of the two fiber types had an influence on specific strength and specific stiffness measured at the same density. The proportion of carbon fibers in the composition of hybrids also had an influence on specific strength and specific stiffness.

Hybrid effect. Compressive strengths of hybrid specimens obtained from the experimental tests were compared to those obtained using RoM, and hybrid effects were calculated. Figure 13(a) to (c) show the compressive strengths obtained from experiments and the RoM versus hybrid ratio. A negative hybrid effect on compressive strength existed for all hybrid specimens with a maximum effect of −32.01% for sample 1 in group I. A minimum negative hybrid effect of −18.08% is observed for sample 3 in group IV. Figure 13(d) shows the hybrid effect on compressive strength for different dispersions versus hybrid ratio.

Hybrid effects on ultimate compressive failure strain were also calculated, and it was observed that specimens in group I were inclined to have the so-called positive hybrid effect, with a maximum effect of +3.22% for sample 3 and +1.61% for samples 1 and

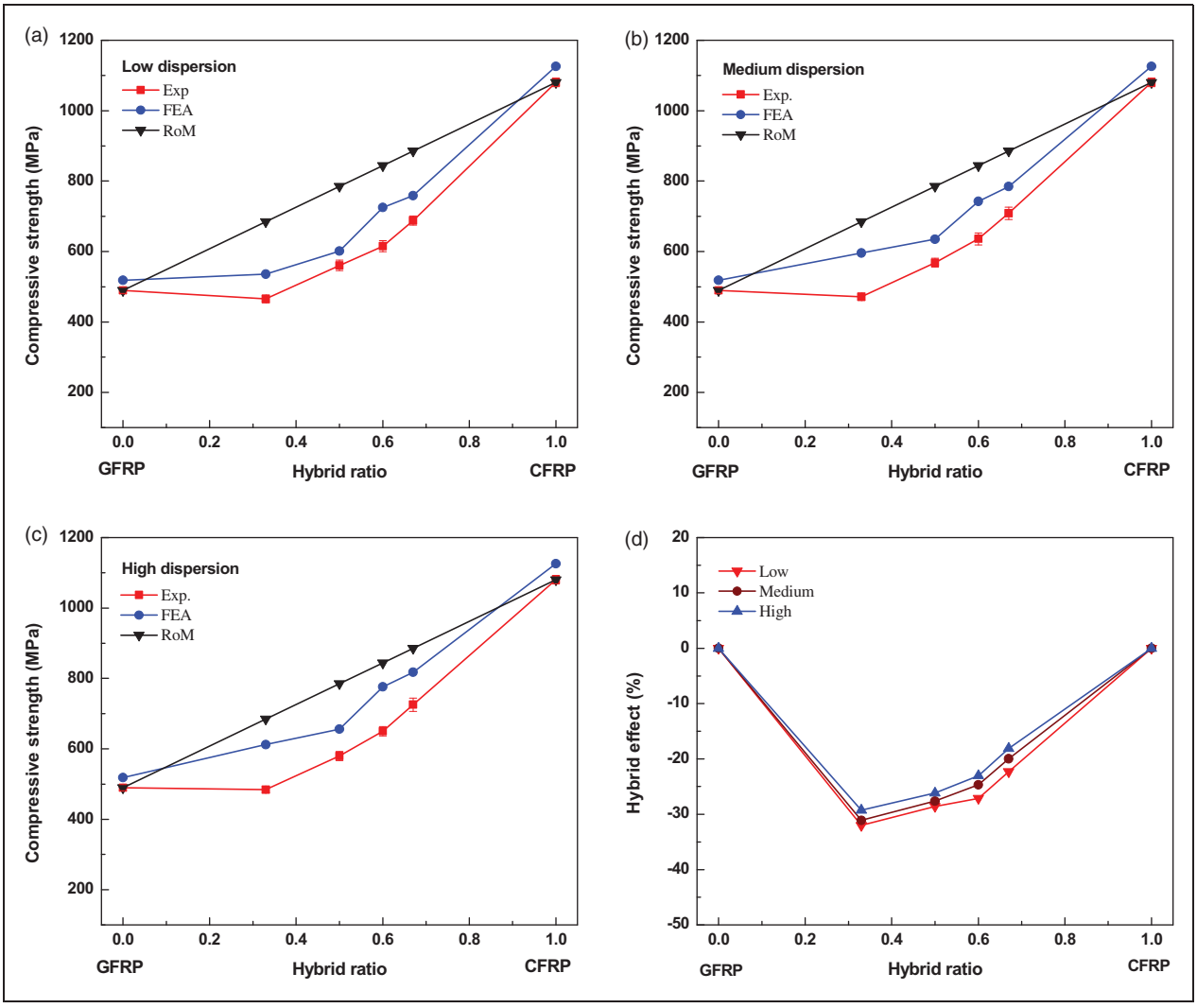

Figure 13. Compressive strengths versus rule-of-mixtures (RoM): (a) low dispersion; (b) medium dispersion; (c) high dispersion. (d) Hybrid effect on compressive strength versus hybrid ratio.

2. Negative hybrid effects on ultimate compressive failure strain were observed for the specimens in groups II, III, and IV. A maximum negative hybrid effect of −12.21% was observed for sample 1 in group II. A minimum negative hybrid effect of −6.86% was found for sample 3 in group III. Figure 14(a) to (c) show the compressive failure strains obtained from experiments and using the RoM versus hybrid ratio. Figure 14(d) plots the hybrid effect on compressive failure strains versus hybrid ratio.

As the proportion of carbon fiber content increases, the hybrid effect for compressive strength and failure strain decreases. Now, the effect of dispersion of the two fiber types on hybrid effect for compressive strength and failure strain is not very significant. A hybridization effect has been monitored in some studies on hybrid composites made of unidirectional layers under compressive loading.[8,57,61,62]

The void content is a critical parameter that could affect the mechanical performance of composites. In many composite applications, the void content is quite critical and levels above about 1% are not tolerable, such as in advanced composite dynamic aerospace structures.[63] In other applications, levels of 5% and higher can be tolerated.[64] In this work, however, the void content of the composites was in the range of 0% to 0.7%, therefore better impregnation was achieved during manufacturing and it could be said that it did not affect the mechanical properties or hybrid effect significantly.

Considering the discussion above, it can be concluded that the tensile and compressive properties such as ultimate strength, strain, modulus, specific strength, and specific stiffness have values between those of CFRP and GFRP depending on the proportion of glass fibers and carbon fibers. Hybridization is a

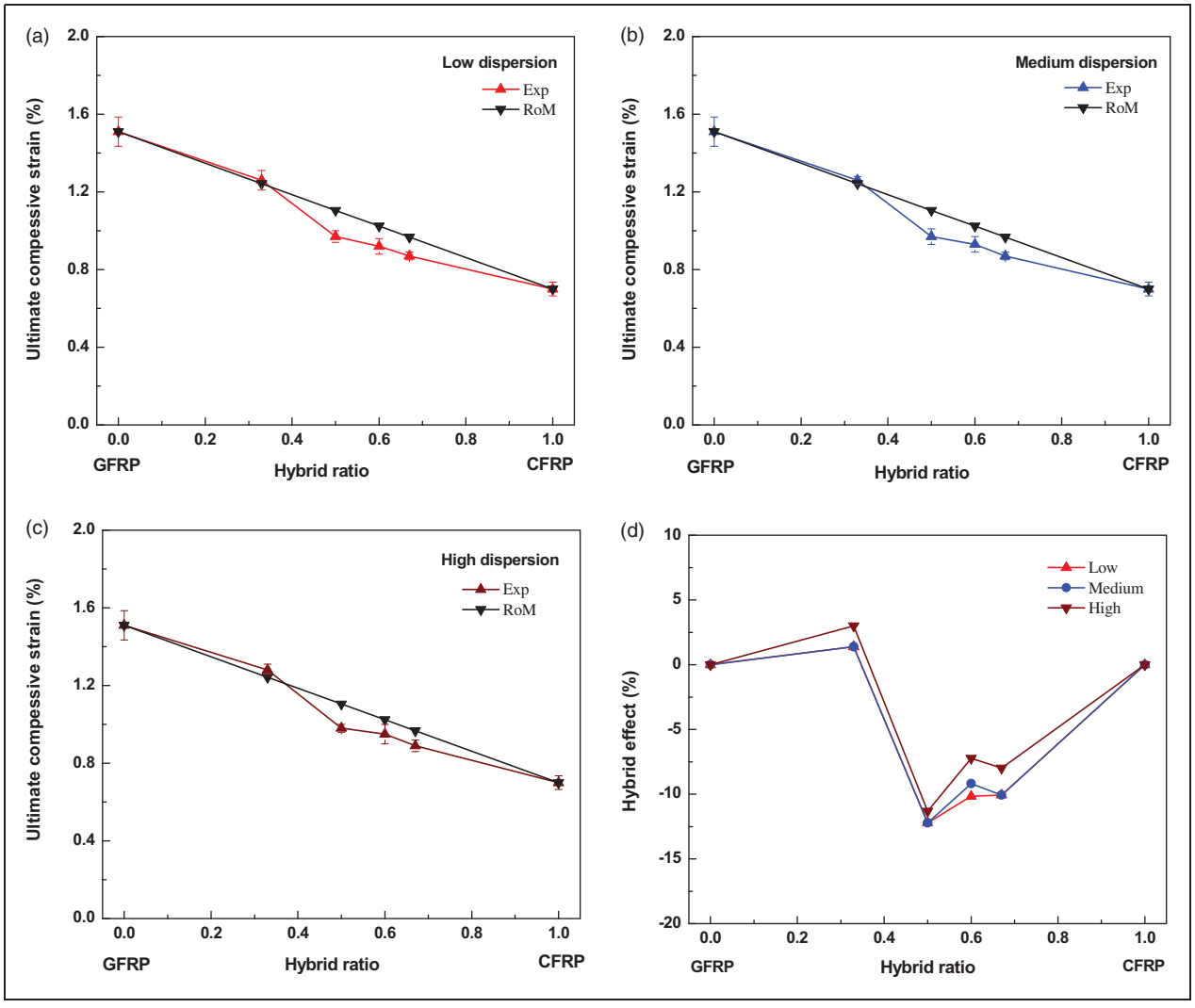

Figure 14. Compressive failure strains versus hybrid ratio: (a) low dispersion; (b) medium dispersion; (c) high dispersion. (d) Hybrid effect on compressive failure strains versus hybrid ratio.

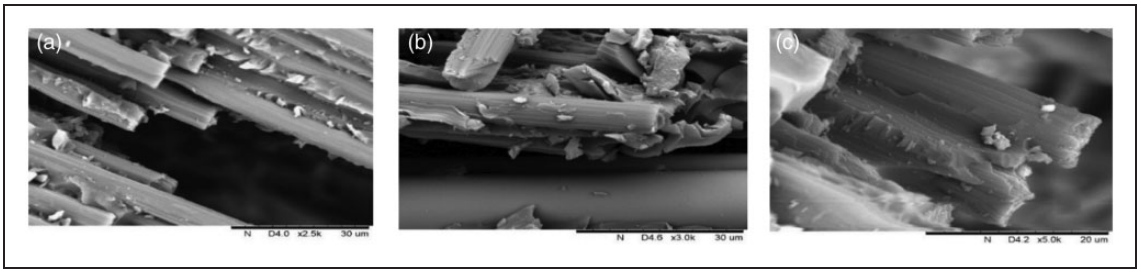

Figure 15. SEM micro-graphs of: (a) damaged surface after tensile test showing irregular fiber breaks (b) fractured surface after compressive loading showing extensive carbon fiber failure (c) Closer view showing excellent bonding between fiber and resin.

trade-off between increase in failure strain and decrease in in-plane strengths, e.g. tensile and compressive strengths of hybrid composites compared with high modulus, low elongation fiber composites. The proportion of carbon fiber plays a significant role in determining the tensile and compressive properties of hybrids. The performance gets even better when the dispersion of the two fiber types improves from low to high. The tensile strength and compressive strength exhibit what is often termed the hybrid effect—for both

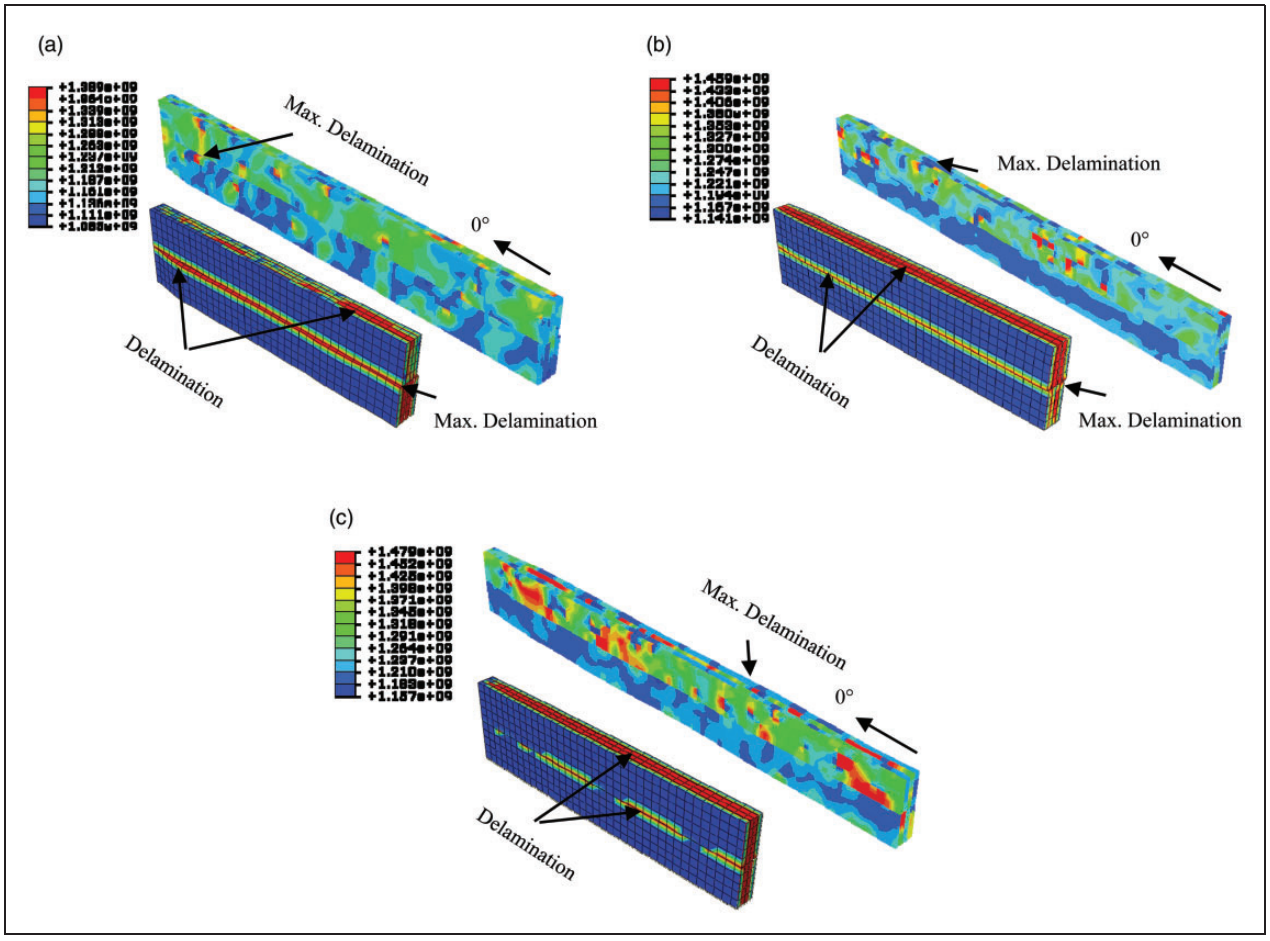

Figure 16. Stress contour and delamination developed after tensile loading in finite element analysis for samples 1, 2, and 3 in group II. (a) C:G, 1:1 (sample 1, low dispersion);(b) C:G, 1:1 (sample 2, medium dispersion);(c) C:G, 1:1 (sample 3, high dispersion).

tensile and compressive strengths, the effect is negative. In terms of tensile and compressive failure strains, the effect is negative for some compositions and positive for some compositions.

Morphological analysis and damage criteria

Morphological analysis of the tested samples was performed using Scanning Electron Microscope (SEM), TM3000, HITACHI, Japan. The samples from tensile and compression tests were studied using SEM. Each sample was dried and sputtered with a layer of gold with a thickness of 15–20 nm using an ion-sputter device (Magnetron Ion Sputter Machine, MSP-IS, Vacuum Device, Inc., US). Figure 15(a) shows the SEM image after the tensile test. The unidirectional orientation of the fibers is clearly seen. The composites exhibit uniform physical properties in longitudinal direction when the fibers are uni-directionally oriented. It shows that there is a non-uniform breakage of fibers, which means that the tensile stress was not distributed uniformly.

The low elongation carbon fiber breaks first, leaving the responsibility to glass fibers to carry out the rest of the load. Figure 15(b) shows the SEM image after the compression test. It is seen that there is a non-uniform breakage of fibers, and again it is the carbon fiber that breaks first. In both SEM images (Figure 15(a) and (b), the bonding between the fiber and the resin is seen, which indicates that the composite is more likely to fail due to breakage of fibers than by debonding of fibers. A closer view shows there is an excellent bonding between fiber and resin (Figure 15(c)).

Non-visible damage to composite structures in a significant concern in many composite industries. To understand the non-visible damage, i.e. delamination occurring at the composites, a cohesive zone model was used. Cohesive behavior is useful in modeling adhesives and bonded interfaces.

Figures 16 and 17 show the damage that occurred to the specimens after being subjected to tensile and compressive loading in FEA. As the stress increased, the fiber and resin cracked progressively across the plane. Significant differences in properties and the glass and

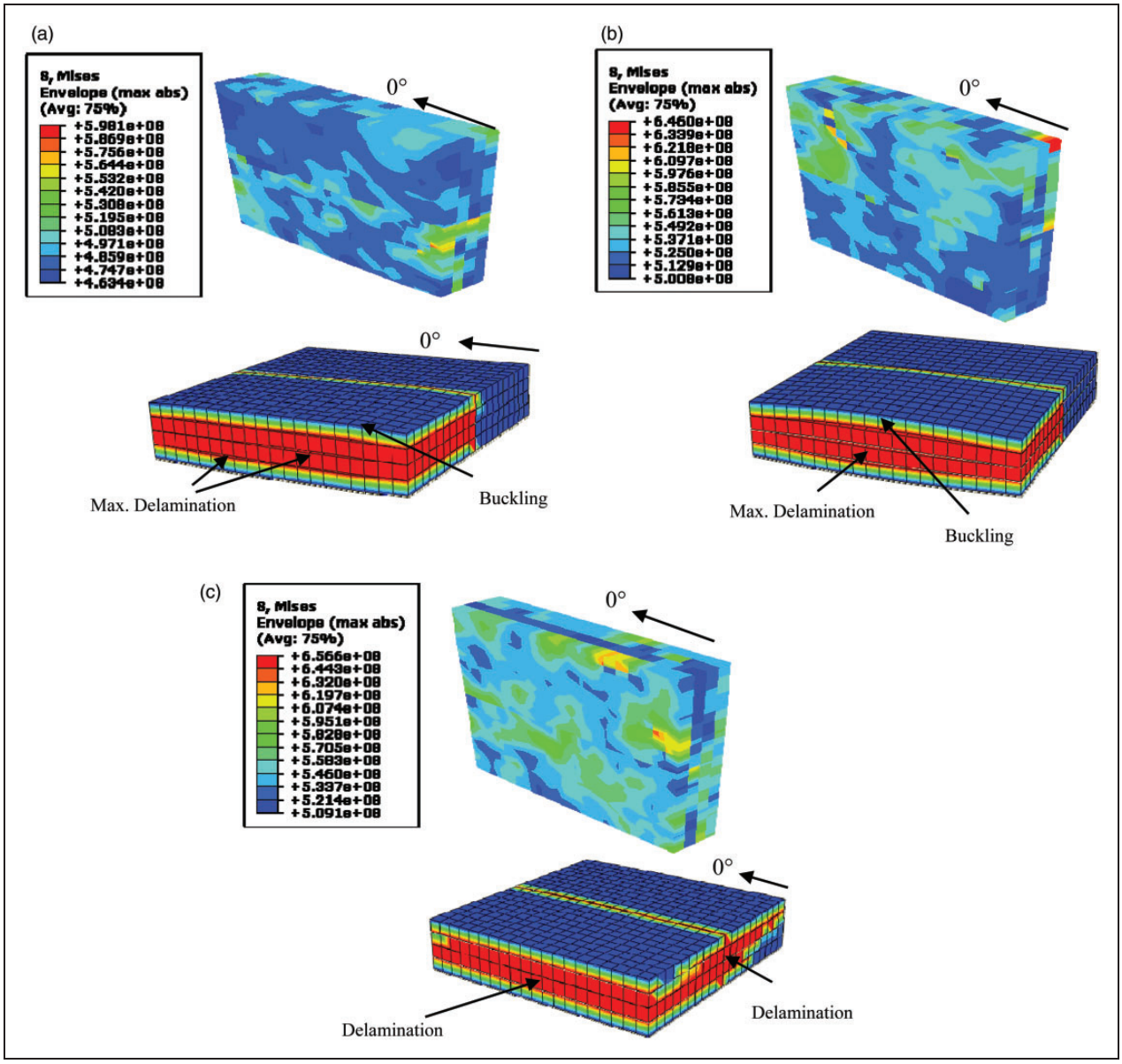

Figure 17. Stress contour and delamination developed after compressive loading in finite element analysis for samples 1, 2, and 3 in group II; (a) C:G, 1:1 (sample 1, low dispersion); (b) C:G, 1:1 (sample 2, medium dispersion); (c) C:G, 1:1 (sample 3, high dispersion).

carbon fiber parts without interlacing led to delamination. The specimen developed delamination at the interfaces between carbon-to-carbon and carbon-to-glass, and the delamination at the interfaces between two dissimilar fibers is more prominent (Figures 16 and 17).

From the plots (Figure 7), it is noticed that all of the composites failed catastrophically. During the experiment, the failure of the carbon fiber parts coincided with the final failure of the hybrid composite and to simplify this no further load carrying by the remaining glass fiber parts was observed. In some experiments however, the authors[11,20,25] examined the remaining load-carrying capacity and behavior of the curves of the remaining glass fibers. It is unclear which parameters are exactly required to maintain this load-carrying capacity after the carbon fiber failure; inter-laminar bonding[11] and dispersion[25] have been proven to play a significant role.

Conclusions

Glass/carbon hybrid composites have been made with different relative proportions of the two fiber types and with different degree of dispersion. Intra-tow hybridization technique has been followed in order to comingle the two fibers in each layer. Tensile and

compressive characteristics of these hybrid laminates have been evaluated and FEA models have been employed to simulate these characteristics. The FEA observations were in good agreement with the experimental results.

In tensile and compression tests, the samples having a higher proportion of carbon fibers exhibited better tensile and compressive properties. With reference to the dispersion of the two fiber types, the samples fabricated with a high degree of dispersion (sample 3) exhibited better performance under quasi-static tensile and compressive loading followed by the samples fabricated with a medium degree of dispersion (sample 2) and then samples made with a low degree of dispersion (sample 1). Samples numbered as samples 1, 2, and 3 in group IV with a similar proportions of the two fiber types (V_{fc}, 0.67; V_{fg}, 0.33) exhibited maximum tensile and compressive strengths. Sample 3 under Group IV exhibited an ultimate tensile strength of 1460.687 MPa and ultimate compressive stress of 725.475 MPa, which were greater than all of the other samples. A significant percentage gain in ultimate tensile strain was noticed and the maximum result was seen for sample 1 in group I, which was a 23.52% enhancement when compared to that of plain carbon/epoxy composite. A maximum enhancement in compressive failure strain was noticed for sample 3 in group I, which was 82.85% when compared to that of plain carbon composite. As the relative proportion of carbon fiber increase, the failure strain enhancement decreases. The so-called hybrid effects exist for tensile and compressive stress, and both hybrid ratio and dispersion have their effects on hybrid effects. A mixed positive and negative hybrid effect exists for both tensile and compressive failure strain. Failure strain enhancement is significant when compared to plain carbon/epoxy.

SEM analysis showed that the low-elongation carbon fiber parts breaks first under tensile and compressive loading. As this happens there is a stress drop noticed in the stress–strain diagram, and the curves again continue extending. This means that the rest of the load is carried by the remaining glass fiber. Therefore, a catastrophic failure of the composite is avoided. Fiber breakage was mainly responsible for the composite failure. In FEA it was observed that the stress began at the two ends of the specimens and the carbon fiber section due to stress concentration, subsequently spreading to somewhere near the center of the specimens. According to Hashin criteria, fiber damage was more prominent in carbon fiber parts due to having a significantly low failure strain. Delamination between the interfaces was observed and it is greater when at the interface between two dissimilar fibers than at the interface between the same fibers.

Declaration of conflicting interests

The authors declared no potential conflicts of interest with respect to the research, authorship, and/or publication of this article.

Funding

The authors disclosed receipt of the following financial support for the research, authorship, and/or publication of this article: This work was supported by the Science and Technology Commission of Shanghai Municipality (Funding No: 15XD1524700) and "Shanghai Municipal Commission of Economy and Informatization (Funding No: CXY-2013-11)".

References

1. Sudarisman DIJ. Flexural failure of unidirectional hybrid fibre-reinforced polymer (FRP) composites containing different grades of glass fibre. *Adv Mater Res* 2008; 41–42: 357–362.
2. Sudarisman DIJ. Influence of compressive pressure, vacuum pressure, and holding temperature applied during autoclave curing on the microstructure of unidirectional CFRP composites. *Adv Mater Res* 2008; 41–42: 323–328.
3. Oya N and Hamada H. Effects of reinforcing fibre properties on various mechanical behaviors of unidirectional carbon/epoxy laminates. *Sci Eng Compos Mater* 1996; 5: 105–130.
4. Oya N and Johnson DJ. Longitudinal compressive behaviour and microstructure of PAN-based carbon fibres. *Carbon* 2001; 39: 635–645.
5. Shioya M and Nakatani M. Compressive strengths of single carbon fibres and composite strands. *Compos Science Technol* 2000; 60: 219–229.
6. Manders P and Bader M. The strength of hybrid glass/carbon fibre composites. *J Mater Sci* 1981; 16: 2233–2245.
7. Zweben C. Tensile strength of hybrid composites. *J Mater Sci* 1977; 12: 1325–1337.
8. Kretsis G. A review of the tensile, compressive, flexural and shear properties of hybrid fibre-reinforced plastics. *Composites* 1987; 18: 13–23.
9. Fischer S and Marom G. The flexural behaviour of aramid fibre hybrid composite materials. *Compos Science Technol* 1987; 28: 291–314.
10. Kalnin I. Evaluation of unidirectional glass–graphite fiber/epoxy resin composites. 1972. Summit, NJ: Celanese Research Co.
11. Bunsell A and Harris B. Hybrid carbon and glass fibre composites. *Composites* 1974; 5: 157–164.
12. Marom G, Fischer S, Tuler FR, et al. Hybrid effects in composites: conditions for positive or negative effects versus rule-of-mixtures behaviour. *J Mater Sci* 1978; 13: 1419–1426.
13. Fu SY, Lauke B, Mader E, et al. Tensile properties of short-glass-fiber-and short-carbon-fiber-reinforced polypropylene composites. *Compos A: Appl S* 2000; 31: 1117–1125.
14. Sudarisman DI. The effects of processing parameters on the flexural properties of unidirectional carbon

fibre-reinforced polymer (CFRP) composites. *Mater Sci Eng: A* 2008; 498: 65–68.
15. Dong C and Davies IJ. Optimal design for the flexural behaviour of glass and carbon fibre reinforced polymer hybrid composites. *Mater Design* 2012; 37: 450–457.
16. Pandya KS, Veerraju C and Naik N. Hybrid composites made of carbon and glass woven fabrics under quasi-static loading. *Mater Design* 2011; 32: 4094–4099.
17. Zhang J, Chaisombat K, He S, et al. Hybrid composite laminates reinforced with glass/carbon woven fabrics for lightweight load bearing structures. *Mater Design* 2012; 36: 75–80.
18. Dong C, Duong J and Davies IJ. Flexural properties of S-2 glass and TR30S carbon fiber-reinforced epoxy hybrid composites. *Polym Composite* 2012; 33: 773–781.
19. Saka K and Harding J. A simple laminate theory approach to the prediction of the tensile impact strength of woven hybrid composites. *Composites* 1990; 21: 439–447.
20. Hayashi T. On the improvement of mechanical properties of composites hybrid composition. *Proc 8th Int Reinf Plas Conf* 1972; paper 22: 149.
21. Zhang Y, Li Y, Ma H, et al. Tensile and interfacial properties of unidirectional flax/glass fiber reinforced hybrid composites. *Compos Science Technol* 2013; 88: 172–177.
22. Chou T and Kelly A. Mechanical properties of composites. *Ann Rev Mater Sci* 1980; 10: 229–259.
23. Shan Y and Liao K. Environmental fatigue behavior and life prediction of unidirectional glass–carbon/epoxy hybrid composites. *Int J Fatigue* 2002; 24: 847–859.
24. Peijs AAJM, Catsman P, Govaert LE, et al. Hybrid composites based on polyethylene and carbon fibres Part 2: Influence of composition and adhesion level of polyethylene fibres on mechanical properties. *Composites* 1990; 21: 513–521.
25. Czél G and Wisnom M. Demonstration of pseudo-ductility in high performance glass/epoxy composites by hybridisation with thin-ply carbon prepreg. *Compos A: Appl S* 2013; 52: 23–30.
26. Aveston J and Sillwood J. Synergistic fibre strengthening in hybrid composites. *J Mater Sci* 1976; 11: 1877–1883.
27. Taketa I, Ustarroz J, Gorbatikh L, et al. Interply hybrid composites with carbon fiber reinforced polypropylene and self-reinforced polypropylene. *Compos A: Appl S* 2010; 41: 927–932.
28. Diao H, Bismarck A, Robonson P, et al. Pseudo-ductile behaviour of unidirectional fibre reinforced polyamide 12 composite by intra-tow hybridization. In: *Proc 5th Eur Conf Compos Mater*, Venice, Italy, June 2012, pp.1–8.
29. You YJ, Park YH, Kim HY, et al. Hybrid effect on tensile properties of FRP rods with various material compositions. *Compos Struct* 2007; 80: 117–122.
30. Swolfs Y, Gorbatikh L and Verpoest I. Fibre hybridisation in polymer composites: A review. *Compos A: Appl S* 2014; 67: 181–200.
31. Chamis C, Lark R and Sinclair J. Mechanical property characterisation of intraply hybrid composites. Test methods and design allowable for fibrous composites. *ASTM STP* 1981; 734: 261–280.
32. Kaw AK. *Mechanics of composite materials*. USA: Taylor & Francis Group, CRC Press LLC, 2005.
33. Grujicic M, Pandurangan B, Koudela KL, et al. A computational analysis of the ballistic performance of light-weight hybrid composite armors. *Appl Surf Sci* 2006; 253: 730–745.
34. Ren P, Zhang Z, Xie L, et al. Hybrid effect on mechanical properties of M40-T300 carbon fiber reinforced Bisphenol A Dicyanate ester composites. *Polym Composite* 2010; 31: 2129–2137.
35. Peijs A and De Kok J. Hybrid composites based on polyethylene and carbon fibres. Part 6: Tensile and fatigue behaviour. *Composites* 1993; 24: 19–32.
36. Bakis CE, Nanni A, Terosky JA, et al. Self-monitoring, pseudo-ductile, hybrid FRP reinforcement rods for concrete applications. *Compos Science Technol* 2001; 61: 815–823.
37. Liang Y, Sun C and Ansari F. Acoustic emission characterization of damage in hybrid fiber-reinforced polymer rods. *J Compos Constr* 2004; 8: 70–78.
38. Pitkethly M and Bader M. Failure modes of hybrid composites consisting of carbon fibre bundles dispersed in a glass fibre epoxy resin matrix. *J Phys D Appl Phys* 1987; 20: 315.
39. Fukunaga H, Chou T-W and Fukuda H. Strength of intermingled hybrid composites. *J Reinf Plast Compos* 1984; 3: 145–160.
40. Goren A and Atas C. Manufacturing of polymer matrix composites using vacuum assisted resin infusion molding. *Arch Mater Sci Eng* 2008; 34: 117–120.
41. Koefoed M. *Modelling and Simulation of the VARTM. Process for Wind Turbine Blades*. Aalborg University, Institute of Mechanical Engineering, Denmark, January 2003.
42. Correia NC, Robitaille F, Long AC, et al. Use of resin transfer molding simulation to predict flow, saturation, and compaction in the VARTM process. *J Fluids Eng* 2004; 126: 210–215.
43. Khattab A. *Exploratory development of VARIM process for manufacturing high temperature polymer matrix composites*. University of Missouri–Columbia, 2006.
44. Boh JW, Louca LA, Choo YS, et al. Damage modelling of SCRIMP woven roving laminated beams subjected to transverse shear. *Composites Part B* 2005; 36: 427–438.
45. Kang M, Lee W and Hahn H. Analysis of vacuum bag resin transfer molding process. *Compos A: Appl S* 2001; 32: 1553–1560.
46. Tzetzis D and Hogg P. Experimental and finite element analysis on the performance of vacuum-assisted resin infused single scarf repairs. *Mater Design* 2008; 29: 436–449.
47. ASTM D3039/D3039M-14. Standard test method for tensile properties of polymer matrix composite materials.
48. ASTM D3171-15. Standard test methods for constituent content of composite materials.
49. ASTM D3410/D3410M-03(2008). Standard test method for compressive properties of polymer matrix composite materials with unsupported gage section by shear loading.
50. Hashin Z. Failure criteria for unidirectional fiber composites. *J Appl Mech* 1980; 47: 329–334.

51. Mishnaevsky L and Dai G. Hybrid carbon/glass fiber composites: Micromechanical analysis of structure–damage resistance relationships. *Comp Mater Sci* 2014; 81: 630–640.
52. Christensen RM. *Mechanics of composite materials*. New York: John Wiley and Sons, 2012.
53. Summerscales J and Short D. Carbon fibre and glass fibre hybrid reinforced plastics. *Composites* 1978; 9: 157–166.
54. Phillips M. Composition parameters for hybrid composite materials. *Composites* 1981; 12: 113–116.
55. Fu SY, Mai YW, Lauke B, et al. Synergistic effect on the fracture toughness of hybrid short glass fiber and short carbon fiber reinforced polypropylene composites. *Mater Sci Eng A* 2002; 323: 326–335.
56. Giancaspro JW, Papakonstantinou CG and Balaguru P. Flexural response of inorganic hybrid composites with E-glass and carbon fibers. *J Eng Mater Technol* 2010; 132: 021005.
57. Hwang S-F and Mao C-P. Failure of delaminated interply hybrid composite plates under compression. *Compos Science Technol* 2001; 61: 1513–1527.
58. Aveston J and Kelly A. Tensile first cracking strain and strength of hybrid composites and laminates. *Philos Trans R So London Ser A* 1980; 294: 519–534.
59. Fukuda H and Chou T. Stress concentrations in a hybrid composite sheet. *J Appl Mech* 1983; 50: 845–848.
60. Pan N and Postle R. The tensile strength of hybrid fibre composites: A probabilistic analysis of the hybrid effects. *Philos Trans R So London Ser A* 1996; 354: 1875–1897.
61. Piggott M and Harris B. Compression strength of hybrid fibre-reinforced plastics. *J Mater Sci* 1981; 16: 687–693.
62. Kouchakzadeh MA and Sekine H. Compressive buckling analysis of rectangular composite laminates containing multiple delaminations. *Compos Struct* 2000; 50: 249–255.
63. Ling Liu B-MZ, Dian-Fu Wang Zhan-Jun and Wu. Effects of cure cycles on void content and mechanical properties of composite laminates. *Compos Struct* 2006; 73: 303–309.
64. Ghiorse SR. Effect of void content on the mechanical properties of carbon/epoxy laminates. *SAMPE J* 1993; 1: 54–59.